NACA RM E51G13

NACA

RESEARCH MEMORANDUM

RELATION OF ENGINE TURBINE-BLADE LIFE TO STRESS-RUPTURE PROPERTIES OF THE ALLOYS, STELLITE 21, HASTELLOY B, CAST S-816, FORGED S-816, X-40, NIMONIC 80, REFRACTALOY 26, N-155, AND INCONEL X

By F. B. Garrett and C. Yaker

Lewis Flight Propulsion Laboratory
Cleveland, Ohio

NATIONAL ADVISORY COMMITTEE
FOR AERONAUTICS

WASHINGTON

August 23, 1951

NACA RM E51G13

2169

NATIONAL ADVISORY COMMITTEE FOR AERONAUTICS

RESEARCH MEMORANDUM

RELATION OF ENGINE TURBINE-BLADE LIFE TO STRESS-RUPTURE PROPERTIES OF THE ALLOYS, STELLITE 21, HASTELLOY B, CAST S-816, FORGED S-816, X-40, NIMONIC 80, REFRACTALOY 26, N-155, AND INCONEL X

By F. B. Garrett and C. Yaker

SUMMARY

An investigation was conducted to determine the relation of engine turbine-blade life to stress-rupture properties of the materials Stellite 21, Hastelloy B, cast S-816, forged S-816, X-40, Nimonic 80, Refractaloy 26, N-155, and Inconel X. Blades of these materials were mounted in a 16-25-6 alloy rotor and subjected to simulated service operation consisting of 20-minute cycles, (15 min at rated speed and approximately 5 min at idle). Stress-rupture tests were conducted on specimens cut from blades to determine the high-temperature strength.

The results of the investigation indicated that the engine blade life of the relatively low-strength alloys, Hastelloy B, N-155, Inconel X, forged S-816, Stellite 21, and Nimonic 80, was predictable on the basis of the stress-rupture properties of the blades alone. The engine blade life of the relatively high-strength alloys, cast S-816, and X-40, Refractalloy 26, fell below the life predicted on the basis of the stress-rupture properties of the blades. In the case of the cast S-816 and X-40, the lowered blade life was attributed to the influence of vibratory stresses in contributing to the failure of the blades. In the case of the Refractaloy 26, the lowered blade life was attributed to corrosion accelerated by the vibratory and thermal stresses in the engine.

INTRODUCTION

The first turbine-blade failure in a jet engine often defines the operating time of the engine to the first overhaul. In an effort to obtain extended blade lives, a number of blade alloys of promising high-temperature properties have been developed. The alloys have been selected as being promising on the basis of standard laboratory tests that determine stress rupture, creep, fatigue, thermal shock, and corrosion properties of alloys at elevated temperatures. In the jet engine, the alloys are subjected to high centrifugal stress, vibratory stresses, thermal stresses, and an oxidizing atmosphere. Performance of alloys of known high-temperature properties under the combined influence



of these conditions is difficult to predict because no laboratory test subjects an alloy to the complex combination of conditions found in service.

For the past several years the NACA Lewis laboratory has been evaluating the performance of gas-turbine-blade alloys by engine operation. This performance will be correlated with data from laboratory tests of the same alloys to establish the high-temperature properties that define engine blade life. As part of this program, blades of nine heat-resistance materials, Stellite 21, Hastelloy B, cast S-816, forged S-816, X-40, Nimonic 80, Refractaloy 26, N-155, and Inconel X, were mounted in a 16-25-6 alloy rotor and operated in a J33-9 turbojet engine. The engine operation consisted of a repetition of a 20-minute cycle (15 min at rated speed and approximately 5 min at idle). Cyclic operation was employed to simulate actual service conditions. At intervals during engine operation, the turbine blades were measured to determine the amount of blade creep and were inspected for damage. The blades were operated to failure. At the conclusion of operation, all blade failures were metallurgically examined to determine the nature of the failure and the structural changes occurring in the blades during operation.

In order to compare the results of the engine operation with laboratory data, the high-temperature strength of the materials was determined. This determination was made by stress-rupture testing of specimens cut from as-received blades. The tests were conducted at the stress and temperature conditions encountered during rated-speed conditions in the engine.

APPARATUS AND PROCEDURE

Temperature control. - In order to make a reliable comparison of the results of engine operation and laboratory data, engine operating conditions had to be so regulated that the turbine blades were operating within a closely controlled range of centrifugal stress and temperature. Of these two variables, temperature is difficult to control, whereas stress is easily controlled by regulating engine speed. Earlier investigators of turbine-blade performance used the gas temperature as measured at the exhaust-cone outlet to control the experimental temperature (references 1 and 2). Changes in burner characteristics, blade twist, and atmospheric conditions during the run, however, would result in different blade temperatures at the same exhaust-cone gas temperature. More accurate blade-temperature regulation is achieved by a control based on the metal temperature itself. In order to control blade temperature during engine operation, thermocouples were therefore inserted in two blades in the rotor. The thermocouple electromotive force is measured

2169

2169

through a slip-ring pickup mounted on the front of the engine. The slip-ring pickup circuit for measuring the temperature is described in reference 3. In order to prevent failure of these blades because of the weakening effect of the hole drilled for the thermocouple, the airfoil section was reduced to one-half the original length to reduce centrifugal stresses in the weakened portion. The thermocouple mounted in the blade is shown in figure 1. The junction of the thermocouple is located 2 inches above the base of the half blades or at the midpoint of a full-length blade. This region is the zone of maximum blade temperature (reference 3). In order to relate the temperature of the half blade to the temperature of a full-length blade, a preliminary investigation was conducted in which temperature measurements were made 2 inches from the base of both half and full-length blades. The results of this survey indicated that at rated speed (11,500 rpm) the temperature of the full-length blade was approximately 25° F higher than that of the half blade.

Turbine blades. - The blade alloys investigated and their chemical compositions are listed in table I. Turbine blades were fabricated from these alloys by commerical methods. The blades were given the following commercial heat-treatments by the fabricator:

Alloy	Heat treatment
Stellite 21	None
Hastelloy B	2 hr at 1900° F, air cooled; 4 hr at 1500° F, air cooled
Cast S-816	None
Forged S-816	1 hr at 2150° F, air cooled; 16 hr at 1400° F, air cooled
X-40	None
Nimonic 80	8 hr at 1925° F, air cooled; 16 hr at 1300° F, air cooled
Refractaloy 26	1 hr at 2100° F, air cooled; 20 hr at 1500° F, air cooled; 20 hr at 1350° F, air cooled
N-155	1 hr at 2250° F, air cooled; 20 hr at 1350° F, air cooled
Inconel X	2 hr at 2100° F, air cooled; 24 hr at 1550° F, air cooled; 20 hr at 1300° F, air cooled

All blades were radiographed for flaws. The 16-25-6 alloy rotor was bladed with 54 blades, two thermocoupled blades and six blades of each alloy except Hastelloy B of which there were only four blades. Prior to engine operation, the cross-sectional areas of each blade were measured on an optical comparator and the stress distributions along the blade were calculated by the method described in reference 4.

2169

Engine operation. - The blades were operated in a J33-9 turbojet engine having a nominal thrust of 4000 pounds and employing a dual-entry centrifugal compressor. The engine has 14 combustion chambers. The engine, fuel, and instrumentation are described in reference 1. The engine investigation consisted of a repetition of the cycle shown in figure 2. During the rated-speed portion of the cycle, the gas temperature was varied to yield an indicated temperature of 1475° ±5° F 2 inches from the base of the half blade. Based on the preliminary investigation, this procedure would result in a temperature of 1500° ±10° F at the midpoint of a full-length blade. The blade temperature was read several times at the beginning of each day's operation to arrive at the proper gas temperature and then checked at regular intervals to assure the maintenance of the correct blade temperature. In figure 2, it is shown that the changes in exhaust-gas temperature during the acceleration and deceleration portions of the test cycle are not reflected in the blade temperature so that no overheating or subcooling of the blades occurs during these stages of the cycle.

Three blades of each material were scribed in the manner shown in figure 3. At regular intervals during engine operation, measurements were made of blade creep between these scribed marks with an optical extensometer having a reading accuracy of ±0.0001 inch. These creep measurements on the turbine blades were made after the blade was cold and the load removed in contrast with laboratory creep measurements, which are made under stress and at temperature. After a failure, the remaining blades were examined for damage resulting from failure of blades or of other engine components and the location and nature of the damage recorded. All blades were operated to failure, which is defined as either complete blade fracture or evidence of the beginning of fracture. In order to minimize the damage resulting from blade fracture, the thickness of the shroud in the engine tail cone surrounding the turbine rotor was reduced to allow blade fragments to pierce the shroud of the tail cone easily and to be thrown clear of the turbine.

Metallurgical examination of blades. - Blade fragments were examined to determine the changes in structure and hardness as a result of engine operation and the nature of the failure propagation. The specimens of the fractured blades were taken from the region of failure and the hardness determinations were made on the transverse surface immediately below the fracture. The examinations were made using standard metallurgical equipment and procedures.

High-temperature strength evaluations. - Stress-rupture tests were conducted on specimens cut from the airfoil sections of blades from the same lots as those used in the engine operation. The shape of the specimen and the zone of the blade from which it was machined are shown in figure 4. The zone of the blade from which the specimen was cut was selected to give a maximum amount of material for a specimen the gage section of which is in the midzone (also the failure zone) of the airfoil section. The stress-rupture tests were all conducted at 1500° F in machines using a loading system, which consisted of a simple beam acting through a system of knife edges. The specimens were heated in a resistance-type furnace. The specimen temperature was so controlled that there was less than a 5° F variation along the length of the specimen with the average temperature varying only ±2° F.

RESULTS AND DISCUSSION

Blade Stresses

From the results of the determinations of the centrifugal stress distributions at rated speed of all experimental blades, the stress for each blade sample at the point of maximum temperature was determined. The average values of this stress for each alloy are listed in table II.

Engine Operation

The wheel containing the experimental blades was operated for a total of 442 cycles or approximately 111 hours at rated speed. Engine operation was concluded at this time because of severe damage to the blades caused by the nozzle diaphragm falling against the wheel. This damage was the result of the failure of the bolts holding the ring and tube assembly in which the nozzle diaphragm was mounted. The nature of the damage to the blades is shown in figure 5. At this point in the investigation, only six of the original blades remained in the wheel. The complete results of the engine operation of the blades are presented in table III. The samples of cast S-816 and N-155 are larger than the original six blades because the early failures of these particular alloys that could be attributed to external damage were replaced with experimental blades from the same lots. Failure time is considered as only the time at rated speed. Because the temperature and stress conditions during the idle portion of the cycle are low, this time is neglected in determining the performance of the blades. All but three alloys, Hastelloy B, Nimonic 80, and Inconel X, had failures that originated in areas of impact damage (table III). There is no quantitative means of evaluating the damage; the interesting qualitative point is the apparently good resistance to damage of Nimonic 80 and Inconel X, the

so-called low-ductility alloys (relative to other forged heat-resistant alloys). In further evaluating the results of the engine operation, the failures resulting from damage will be omitted because they are the result of extraordinary operating conditions and therefore are not indicative of the true performance of an alloy. The order of failure as listed in table III for some of the alloys may not be significant. Since this investigation was initiated turbine blades of some of these alloys have been improved because of changes in fabrication and heat-treatment methods.

The results of the blade-creep measurements indicate that the zone of maximum creep lay just above or below the middle of the blade airfoil section. The elongation distribution along a Hastelloy B blade typical of most of the alloys is shown in figure 6. For this blade, the maximum elongation occurred in section 3, which is just below the middle of the blade. In general, however, the section of maximum elongation was either 3 or 4, the sections just below or above the middle of the blades. In figure 7, the creep curves for sections 3 and 4 are plotted for all the scribed blades that had true failures (not the result of damage). The creep behavior of the alloys, Stellite 21, Hastelloy B, cast S-816, forged S-816, X-40, and N-155, can be considered normal as the curves are normal in shape. The alloys, Nimonic 80, Refractalloy 26, and Inconel X, did exhibit anomalous behaviors because for all three alloys negative values of creep were measured. The alloys, Refractaloy 26, and Inconel X, also showed a rapid increase in elongation sometime between 20 and 30 hours of operation. A possible explanation is that the unusual creep was the result of structural changes occurring in these alloys during engine operation. It may be significant that all three alloys are the so-called age-hardenable type containing titanium and will age at 1500° F. The alloys may age during engine operation by a reaction that results in negative creep. In the cases of Refractaloy 26 and Inconel X overaging may occur, which results in very rapid elongations until the structure stabilizes, possibly as a result of strain hardening. The possibility that the sudden stretch in the Refractaloy 26 and Inconel X blades was due to overtemperature during operation was discounted because the engine-operation data did not indicate any such conditions and the effect was not evident in other alloys. Some corroboration of the suggested cause of the anomalous creep behavior of these alloys may be found in the results of the metallurgical examination presented later.

The final blade elongations in zones 3 and 4 prior to failure for true blade failures plotted in figure 7 are listed in table IV. The values given in table IV are those measured at the shutdown time just before failure. Because of the limited number of blades in each sample, no definite conclusion can be made about blade elongation as compared with blade life. One of the significant points in the curves is the

relatively short third-stage portion of the creep curve and in some cases the absence of all evidence of third-stage creep. The elongation at the point of initiation of third-stage creep appears to be the point of importance in blade creep because failure occurs shortly after the blades have stretched to this elongation.

Metallurgical Examination

The results of the metallurgical examination are presented in figures 8 to 16, which present the nature of the blade failures on a macroscopic and microscopic scale, the changes in structure during operation, and for the forged alloys, the grain size of the blades. No metallurgical examination of the Hastelloy B blades is included in this report because the nature of the blade failures and structural changes are the same as those described in reference 5. In all cases the micrographs shown are those believed typical of the entire blade sample both as to nature of failure and structure before and after operation. The results of the metallurgical examinations of the blade failures indicate that the failures were of the following three types:

(1) Failures in which the origin of the fracture is characterized by an irregular granular surface having no evidence of fatigue-type failure. The fracture has an intercrystalline path and small intercrystalline cracks are present in the area just below the failure zone. Because of the similarity of failures of this type to those encountered in laboratory stress-rupture investigations, these failures were classed as the stress-rupture type.

(2) Failures characterized by a smooth fracture surface at the failure origin sometimes showing the familiar concentric ring markings of a fatigue failure. These failures have a transcrystalline path. In this class, fall the failures that are the result of the combined effects of the centrifugal and vibratory stresses and show no evidence of initiation of the stress-rupture-type failure. These failures will be classed as the fatigue type.

(3) Failures in which the fracture was initiated in a zone similar to that described for the stress-rupture-type failure. The failure then progressed through a zone of the fatigue-type failure. The stress-rupture origin of these failures is determined by macroscopic and microscopic examination of both the initial cracks detected during operation and the final fracture. These failures will be classed as the stress-rupture-followed-by-fatigue type.

The preceding classifications refer only to the beginning zones of blade failure. After fracture has progressed to a critical depth by any of the foregoing types of failure, the blades fail in tension because of the high stresses produced by the reduced load-carrying area. In figure 16, the results of the engine operation are presented showing the type of failure mechanism associated with each true blade failure (failure initiated by mechanical damage is considered not a true blade failure). Some confirmation of the accuracy of the failure classifications will be found in the comparison of the results of the engine and stress-rupture tests presented later in this report. Metallurgical examination of the blades did not indicate any significant differences in structure between the first and last blades of each alloy to fail.

No comparison could be made between the structures of the previously fractured blades and the blades still in operation at the conclusion of the investigation. The remaining blades were overheated in the engine failure that ended the test. This is evidenced by the recrystallization at the zone of damage in an Inconel X blade (fig. 17).

The results of the change in hardness during operation are summarized in table V. The hardness before operation was determined on the remaining pieces of the blades from which the stress-rupture specimens were machined. These results indicate that the hardness of all the cast alloys was increased by engine operation. This increase probably was the result of precipitation (figs. 8(e), 9(d), and 11(d)). Of the forged alloys, S-816 and N-155 both increased in hardness during operation but precipitation was visible in only the N-155 (fig. 14(f)); Nimonic 80, Refractaloy 26, and Inconel X all decreased in hardness during operation with increased precipitation visible in the Nimonic 80 and Inconel X (figs. 12(e) and 15(e)) but not in the Refractaloy 26 (fig. 13(e)). The decrease in hardness of these alloys indicates that overaging has apparently occurred during engine operation. In the case of the Refractaloy 26 and Inconel X, this overaging is the probable cause of the sudden increases in blade elongation previously reported. Nimonic 80 probably did not show the same increase because the decrease in hardness for this alloy was less than for Refractaloy 26 and Inconel X. A lesser degree of overaging may therefore not have resulted in as severe a loss in strength or the decrease may have occurred just before failure of the alloy. If the decrease occurred then it would not be noted in the creep curves. As stated before, the Nimonic 80, Refractaloy 26, and Inconel X are all age-hardenable alloys containing titanium, which is perhaps a clue to their unusual creep behavior.

Correlation of Results

The results of the stress-rupture tests from blade specimens and blade life in the engine are compared in figure 18. The blade-failure times are plotted at the average stress levels shown in table II. Included in figure 18 are the stress-rupture curves for bar stock of the same lots (reference 6) from which the blades were fabricated for all alloys except Stellite 21 and Hastelloy B. For these two alloys, the manufacturer's data were used. For the cast alloys, the strength of the blades is nearly equal to or just above that of the bar stock. The slight strength differences between the cast bar stock and the blades was probably due to the heat-treating of the bars, whereas the blade specimens were tested in the as-cast condition. For the forged alloys, the strength of the blades is below that of the bar stock for the alloys, S-816, Nimonic 80, and Refractaloy 26, approximately equal to the bar stock for Inconel X and Hastelloy B, and above that of the bar stock for only N-155. These results indicate that only the N-155 has been improved by forging into blades. The results of the blade failures in the engine fall within the bands drawn through results of the blade-specimen stress tests for the alloys, Stellite 21, Hastelloy B, forged S-816, Nimonic 80, and Inconel X. For cast S-816, X-40, Refractaloy 26, and N-155, some or all the blade failures fall below the bands for the blade specimens.

In figure 19, the stress-rupture life of the blades as determined from blade specimens is compared with the blade life in the engine. In figure 19(a), the comparison is made on the basis of the minimum blade life and the minimum stress-rupture life; also the data points are classified as to type of initial blade failure encountered. There is no minimum point for Hastelloy B because all failures occurred at the same time and are plotted as an average point in a later figure. This curve indicates that for the alloys, N-155, Inconel X, forged S-816, Stellite 21, and Nimonic 80, the minimum blade life can be predicted with a fair degree of accuracy from stress-rupture tests on blade specimens. The Stellite 21 and Nimonic 80 points lie above the line of 1:1 correlation, indicating higher minimum blade life than that predicted by the stress-rupture tests. This anomaly is probably the result of both the relatively small sample, which did not accurately define the minimum blade life and, in the case of Stellite 21, the grain-orientation effect in the blade specimen. The three alloys that had significantly lower minimum blade life than that predicted by the blade-specimen stress rupture were cast S-816, Refractaloy 26, and X-40.

The average blade life is compared with the average blade-specimen stress-rupture life in figure 19(b). The failure types for each alloy shown in figure 19(b) are those most characteristic of that alloy. In

this case, the alloys, Hastelloy B, N-155, forged S-816, Stellite 21, and Nimonic 80, conform to the line of 1:1 correlation, whereas the alloys, cast S-816 and Refractaloy 26, fall considerably below the line. No average points were plotted for Inconel X and X-40 because some of the blades of these alloys were still intact at the conclusion of the engine investigation. From these two plots (fig. 19) discounting the high minimum blade life of the Stellite 21 and Nimonic 80, prediction of blade life with accuracy could be made on the basis of the stress-rupture strength of the blades for the alloys of relatively low blade-specimen strength (short life (fig. 18)), that is, Hastelloy B, N-155, Inconel X, forged S-816, Stellite 21, and Nimonic 80. The vibration and cyclic operation apparently do not decrease the life of these alloys. These results also confirm the classification of the failure types for these alloys because they were all either of the stress-rupture or stress-rupture-followed-by-fatigue type. In reference to the stress-rupture-followed-by-fatigue-type failure, the results indicate that the fatigue mechanism only propagates the fracture of the alloys after the start as the result of the stress-rupture-type failure. The alloys that had blade lives appreciably lower than those predicted by the stress-rupture tests of the blade specimens were the relatively higher blade-specimen strength (short life (fig. 18)) alloys, cast S-816, X-40, and Refractaloy 26. For the cast S-816, and X-40, the low blade life can be explained by the failure of these alloys through a fatigue-type fracture, which indicates that their blade life is shortened by vibratory stresses. The Refractaloy 26, however, is anomalous in that examination of the failures indicated that they apparently had the characteristics of a stress-rupture failure. A possible answer to why the Refractaloy 26 blades failed in less time than predicted by stress-rupture test can be found in the nature of the oxide film on the blades. In figure 20(a), a tightly adherent oxide film, which formed on the blades during engine operation, is visible. In figures 20(b) and 20(c), this same oxide film appears to be penetrating along the grain boundaries of the blade and is visible along the fracture surface of the blade. In the stress-rupture test, the oxide film, which is apparently quite adherent, probably penetrates into the grain boundary very slowly and the oxidation does not appreciably contribute to the failure of the alloy. Under the influence of vibratory stresses and the alternate heating and cooling in the engine, however, this tight oxide film would be broken by the reversal of stresses further exposing the surface of the metal so that penetration would proceed more rapidly with a resultant reduction in alloy strength (shorter life).

SUMMARY OF RESULTS

The investigation of turbojet-engine performance and laboratory stress-rupture properties of turbine blades of the heat-resistant alloys, Stellite 21, Hastelloy B, cast S-816, forged S-816, X-40, Nimonic 80, Refractaloy 26, N-155, and Inconel X showed that:

1. The engine life for the blades of the relatively low-strength alloys, Hastelloy B, N-155, and Inconel X, forged S-816, Stellite 21, and Nimonic 80 was predictable on the basis of the stress-rupture properties of the blades alone. Blades of these alloys all failed by either a stress-rupture or a stress-rupture followed by fatigue-type failure and were not appreciably affected by the cyclic operation or the vibratory stresses.

2. The engine life for the blades of the relatively high strength alloys, cast S-816, X-40 and Refractaloy 26, fell below the life predicted on the basis of the stress-rupture properties of the blades. In the case of the cast S-816 and X-40 blades, the low life was attributed to the influence of vibratory stresses in contributing to the failure of the blades. In the case of the Refractaloy 26 blades, the low life was attributed to corrosion accelerated by the vibratory and thermal stresses in the engine.

Lewis Flight Propulsion Laboratory,
National Advisory Committee for Aeronautics,
Cleveland, Ohio, February 21, 1951.

REFERENCES

1. Farmer, J. Elmo, Darmara, F. N., and Poulson, Francis D.: Cyclic Engine Test of Cast Vitallium Turbine Buckets - I. NACA RM E7J23, 1948.

2. Farmer, J. Elmo, Deutsch, George C., and Sikora, Paul F.: Cyclic Engine Test of Cast Vitallium Turbine Buckets. - II. NACA RM E7J24, 1948.

3. Farmer, J. Elmo: Relation of Nozzle Blade and Turbine-Bucket Temperatures to Gas Temperatures in a Turbojet Engine. NACA RM E7L12, 1948.

4. Kemp, Richard H., and Morgan, William C.: Analytical Investigation of Distribution of Centrifugal Stresses and Their Relation to Limiting Operating Temperatures in Gas-Turbine Blades. NACA RM E7L05, 1948.

5. Yaker, C., Robards, C. F. and Garrett, F. B.: Investigation of Mechanisms of Blade Failure of Forged Hastelloy B and Cast Stellite 21 Turbine Blades in Turbojet Engine. NACA RM E51D16, 1951.

6. Fields, Melvin E., and Rector, W. H.: Investigation of the Stress Rupture Properties at 1500° F of a number of High Temperature Alloys. Tech. Rep. No. 5893, Air Materiel Command, July 1949.

2169

TABLE I - CHEMICAL COMPOSITION OF BLADE-ALLOYS INVESTIGATED

[All compositions are actual except that for Stellite 21, which is nominal.]

Alloy	Chemical composition (percent)											
	C	Ni	Co	Cr	Mo	W	Cb	Ti	Fe	Mn	Si	Other
[a]Stellite 21	0.25	2.75	bal	27.0	5.5	----	----	----	1.0	0.60	0.60	--------
[b]Hastelloy B	.03	bal	-----	.05	28.72	----	----	----	4.36	.60	.27	--------
[b]Cast and	.35	19.18	44.10	20.32	4.17	4.13	3.57	----	2.51	.78	.23	--------
forged S-816	.40	20.68	43.40	19.79	3.46	4.46	3.80	----	2.50	.70	.51	--------
[b]X-40	.50	10.13	bal	26.18	-----	7.37	----	----	2.00	.72	.61	--------
[b]Nimonic 80	.05	74.23	-----	20.33	-----	----	----	2.56	.73	.64	.63	0.78 Al, .02 Cu
[b]Refractaloy 26	.059	37.50	20.50	18.00	2.90	----	----	2.97	16.10	.80	.84	.14 Al
[b]N-155	.19	18.99	19.35	21.53	3.00	2.22	1.18	----	bal	1.26	.57	.11 N_2
[b]Inconel X	.04	73.62	-----	14.62	-----	----	1.03	2.38	6.56	.56	.42	.68 Al, .03 Cu

[a]Nominal composition.

[b]Actual composition.

2169

TABLE II - AVERAGE CENTRIFUGAL STRESS AT 11,500 rpm IN TURBINE BLADES AT POINT OF MAXIMUM TEMPERATURE[a]

Alloy	Stress (lb/sq in.)
Stellite 21	20,700
Hastelloy B	25,000
Cast S-816	21,800
Forged S-816	21,500
X-40	21,500
Nimonic 80	21,000
Refractaloy 26	20,500
N-155	21,000
Inconel X	21,000

[a]Determined 2 in. above base of blade.

2169

TABLE III - RESULTS OF ENGINE OPERATION OF TURBINE BLADES

Alloy	Order of failure	Failure time at rated speed (hr)	Failure time at rated speed (cycles)
Stellite 21	[a]1	30.0	120
	[a]2	42.0	168
	3	46.0	184
	[a]4	50.7	$202\frac{16}{20}$
	5	63.0	252
	6	73.2	$292\frac{17}{20}$
Hastelloy B	1	15.0	60
	2	15.0	60
	3	15.0	60
	4	15.0	60
Cast S-816	[a]1	5.7	$22\frac{17}{20}$
	2	51.7	$206\frac{17}{20}$
	[a]3	61.0	$244\frac{11}{20}$
	4	100.1	$400\frac{12}{20}$
	5	100.1	$400\frac{12}{20}$
	[a]6	101.9	$407\frac{18}{20}$
	7	109.4	$437\frac{16}{20}$
Forged S-816	[a]1	33.6	$134\frac{11}{20}$
	2	34.8	$139\frac{6}{20}$
	3	44.1	$176\frac{9}{20}$
	4	44.7	$178\frac{17}{20}$
	5	44.7	$178\frac{17}{20}$
	6	49.4	$197\frac{16}{20}$
X-40	[a]1	63.0	252
	[a]2	63.0	252
	[b]3	99.4	$398\frac{13}{20}$
Nimonic 80	1	52.8	$211\frac{7}{20}$
	2	66.9	$267\frac{13}{20}$
	3	70.0	$279\frac{19}{20}$
	4	74.3	$297\frac{7}{20}$
	5	82.2	$328\frac{18}{20}$
	6	82.9	$331\frac{14}{20}$
Refractaloy 26	[a]1	60.6	$242\frac{8}{20}$
	[a]2	67.5	$269\frac{17}{20}$
	3	67.5	$269\frac{17}{20}$
	4	70.3	$281\frac{7}{20}$
	5	71.8	$287\frac{15}{20}$
	6	85.0	340
N-155	[a]1	9.0	36
	[a]2	17.1	$68\frac{8}{20}$
	3	20.3	$81\frac{8}{20}$
	4	22.2	$88\frac{18}{20}$
	5	24.8	$99\frac{9}{20}$
	6	24.8	$99\frac{9}{20}$
	7	27.0	108
	8	35.1	$140\frac{9}{20}$
Inconel X	1	30.2	$120\frac{9}{20}$
	2	57.8	$231\frac{9}{20}$
	[b]3	92.6	$370\frac{11}{20}$

[a]Caused by damage.
[b]Remaining blades were still in operation at conclusion of investigation.

2169

TABLE IV - BLADE ELONGATION IN ZONES OF MAXIMUM ELONGATION PRIOR TO FAILURE

Alloy	Failure time (hr)	Elongation in 1/2 in. (percent)	
		Section 3[a]	Section 4[b]
Stellite 21	63.0	2.70	2.25
Hastelloy B	15.0	4.70	3.53
	15.0	5.00	3.45
	15.0	5.30	3.37
Cast S-816	100.1	2.24	2.43
	109.4	2.62	3.05
Forged S-816	44.7	1.81	2.50
	49.4	3.25	3.07
X-40	99.4	2.30	1.74
	[c]110.5	2.80	2.47
	[c]110.5	2.94	3.14
Nimonic 80	52.8	0.80	----
	74.3	-.50	0.85
	82.2	.00	1.27
Refractaloy 26	70.0	1.50	1.97
	85.0	1.00	1.65
N-155	20.3	4.20	2.57
	27.0	4.20	4.05
	35.1	2.25	2.35
Inconel X	30.2	1.08	1.75
	92.6	2.35	5.00
	[c]110.5	.88	2.24

[a] $1\frac{3}{8}$ to $1\frac{7}{8}$ in. from blade base.

[b] $1\frac{7}{8}$ to $2\frac{3}{8}$ in. from blade base.

[c] Still in operation at conclusion of investigation.

TABLE V - CHANGE IN HARDNESS DURING ENGINE OPERATION

Alloy	Average Rockwell-A hardness at failure zone		
	Before operation	After operation	Change
Stellite 21	65.5	71.0	5.5
Cast S-816	61.5	66.2	4.7
Forged S-816	63.5	65.1	2.6
X-40	64.6	71.0	6.4
Nimonic 80	64.1	63.2	-0.9
Refractaloy 26	65.0	63.0	-2.0
N-155	59.6	61.2	1.6
Inconel X	64.2	60.7	-3.5

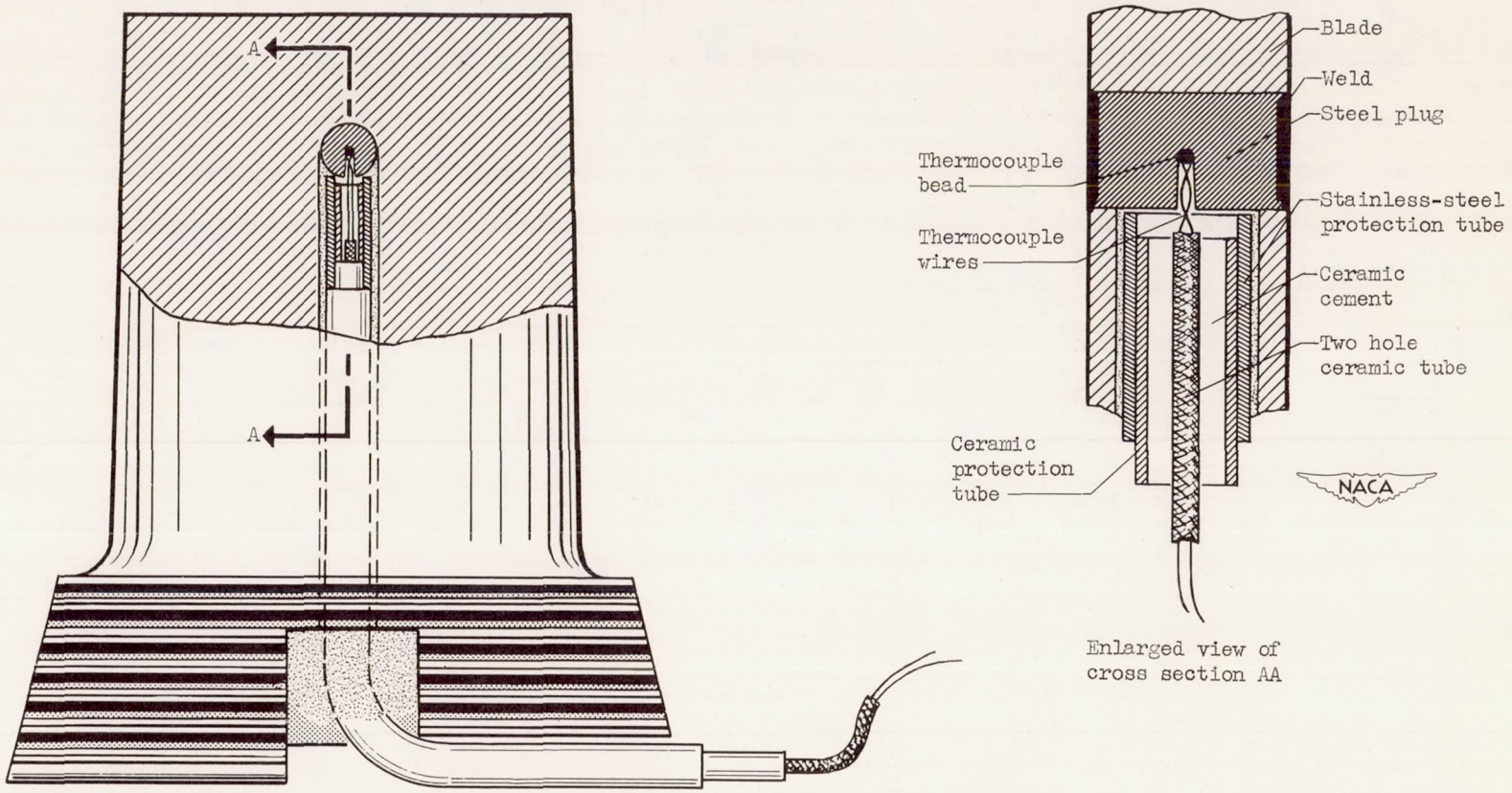


Figure 1. - Thermocouple installation in half blade.

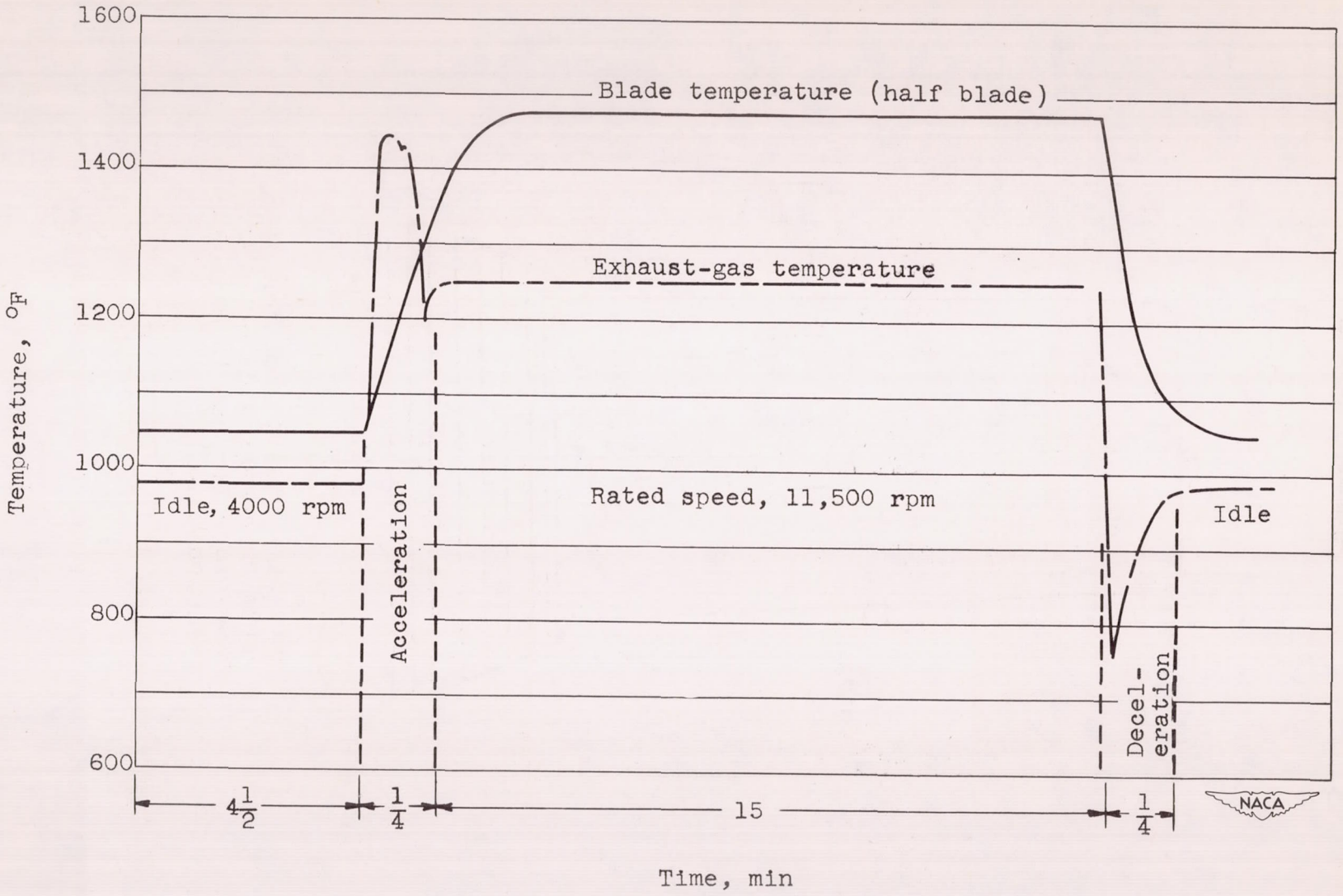


Figure 2. - Temperature conditions during typical engine cycle.

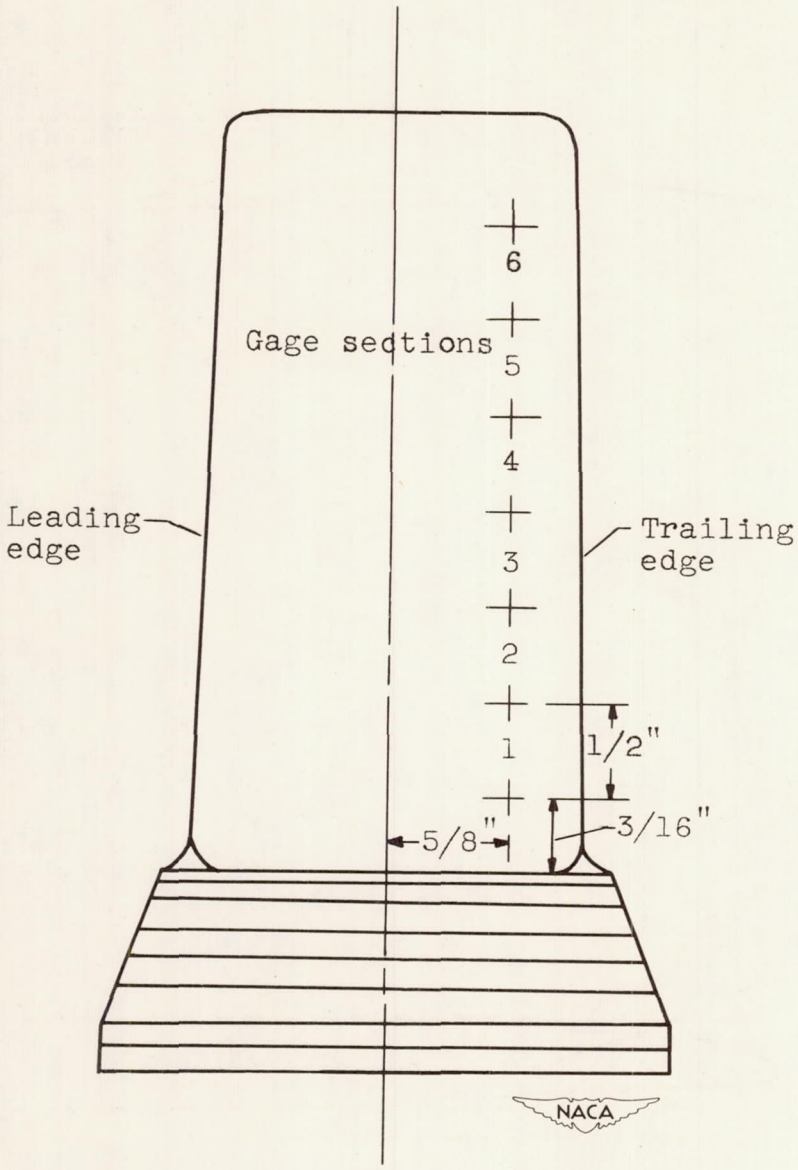


Figure 3. - Location of scribe marks on convex side of turbine blade for use in measuring elongation.

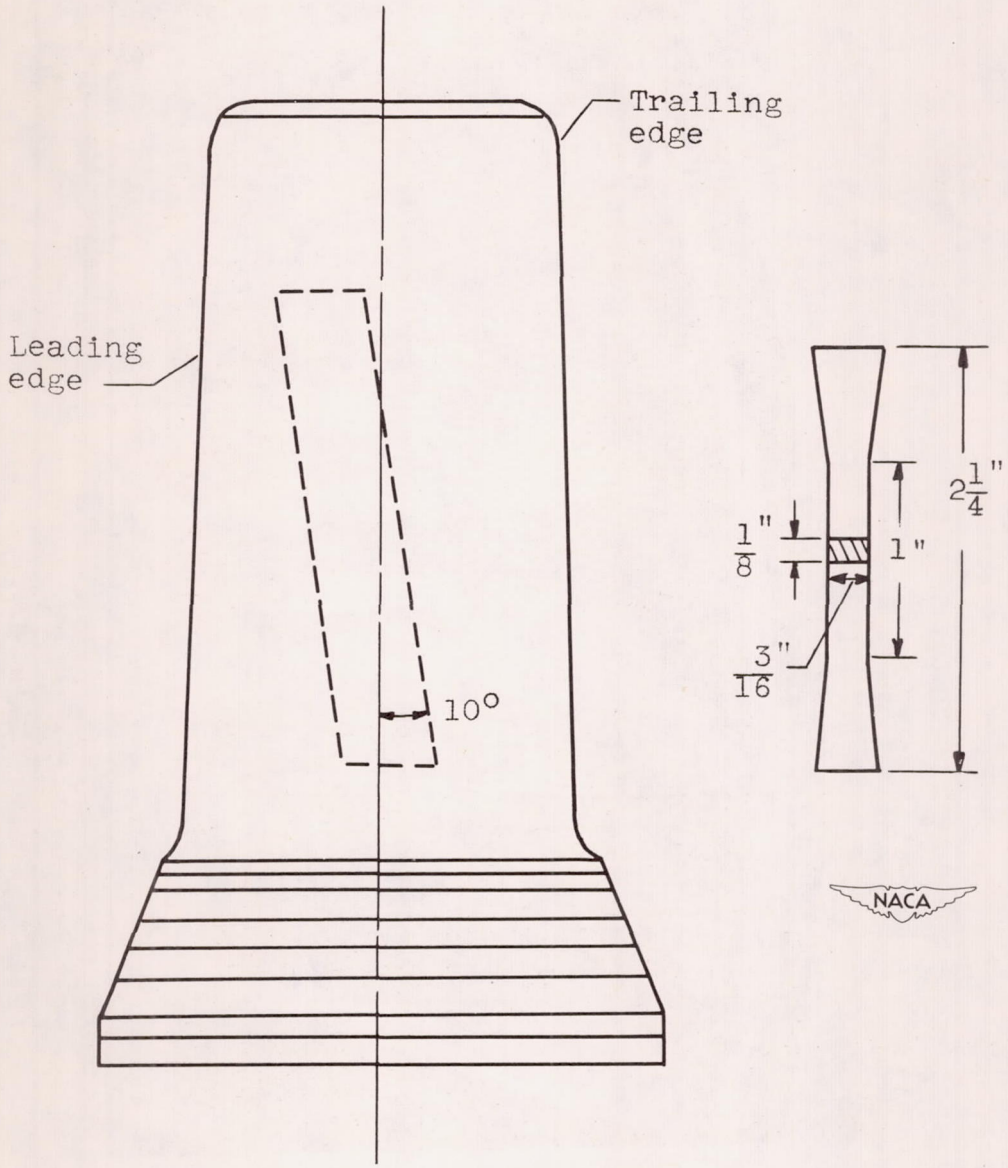


Figure 4. - Blade stress-rupture specimen and zone from which it was machined.

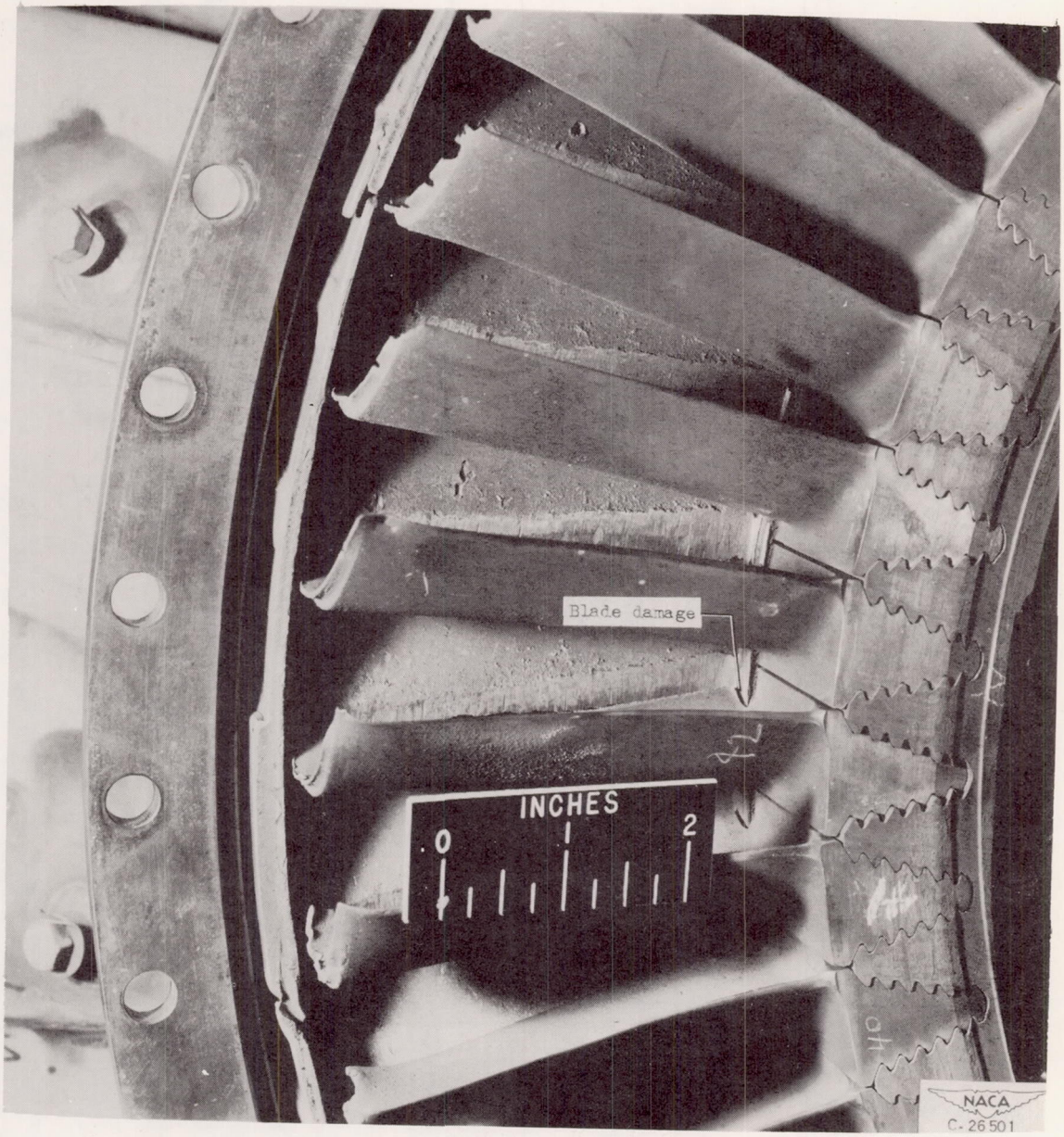


Figure 5. - Damaged turbine blades resulting from nozzle diaphragm falling against turbine.

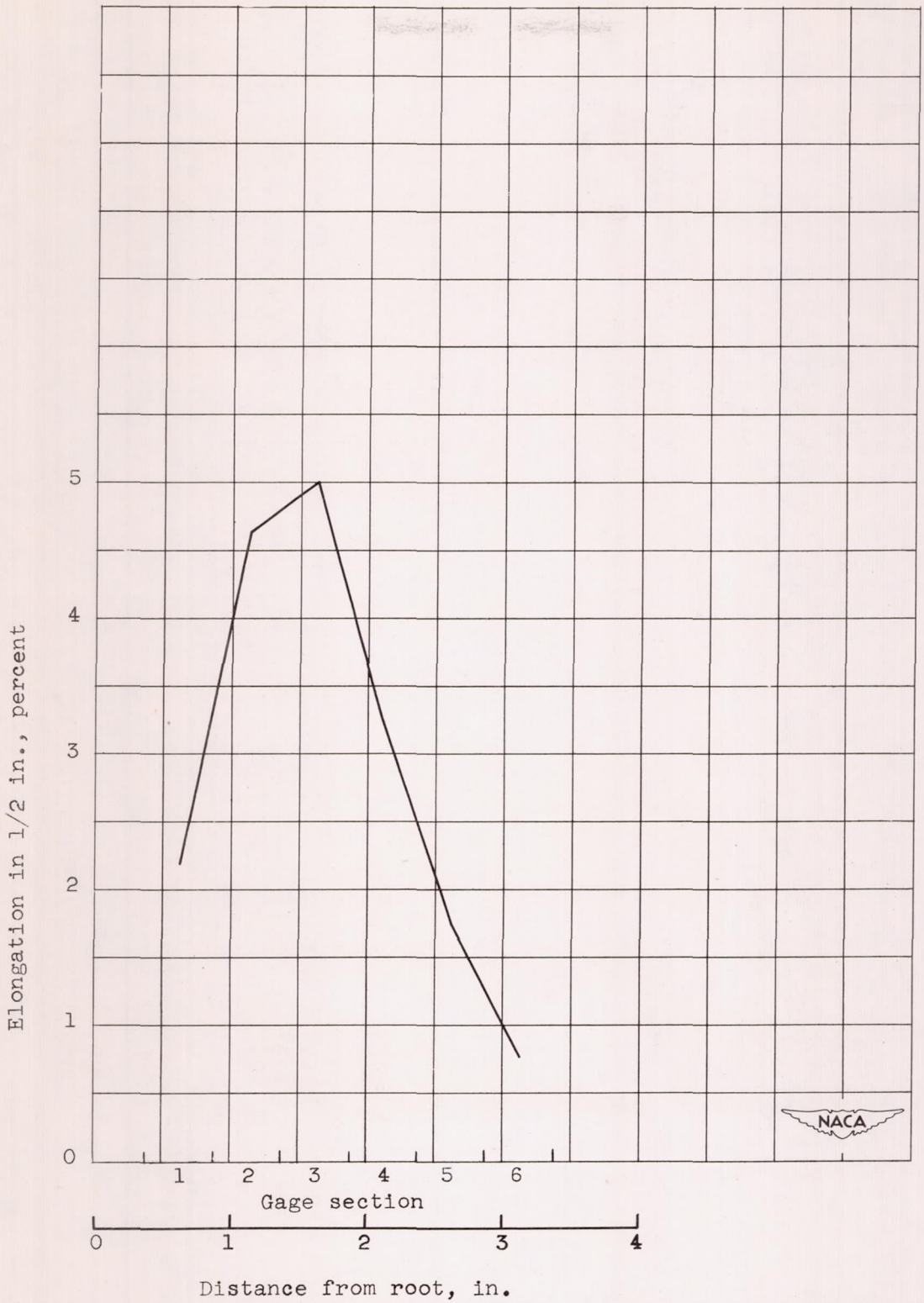
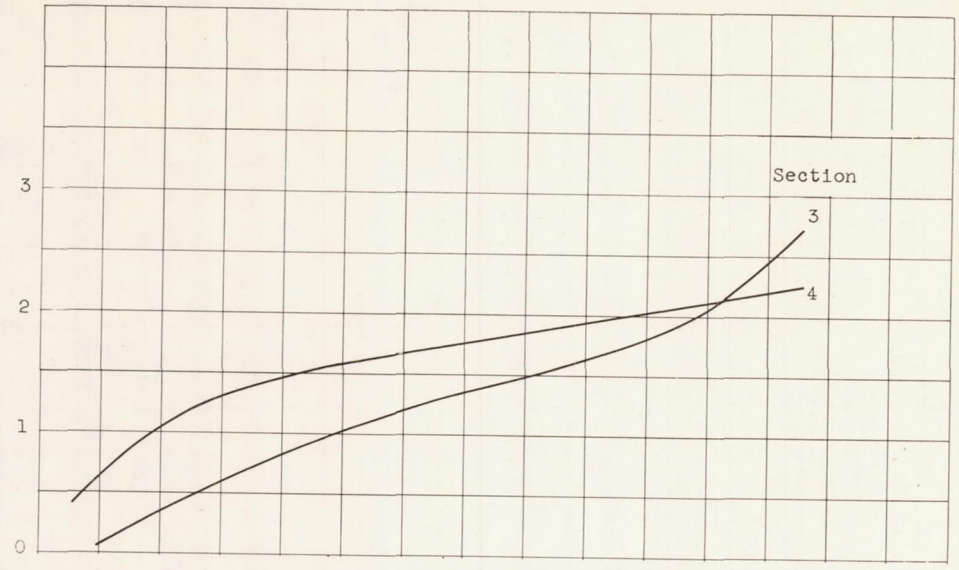
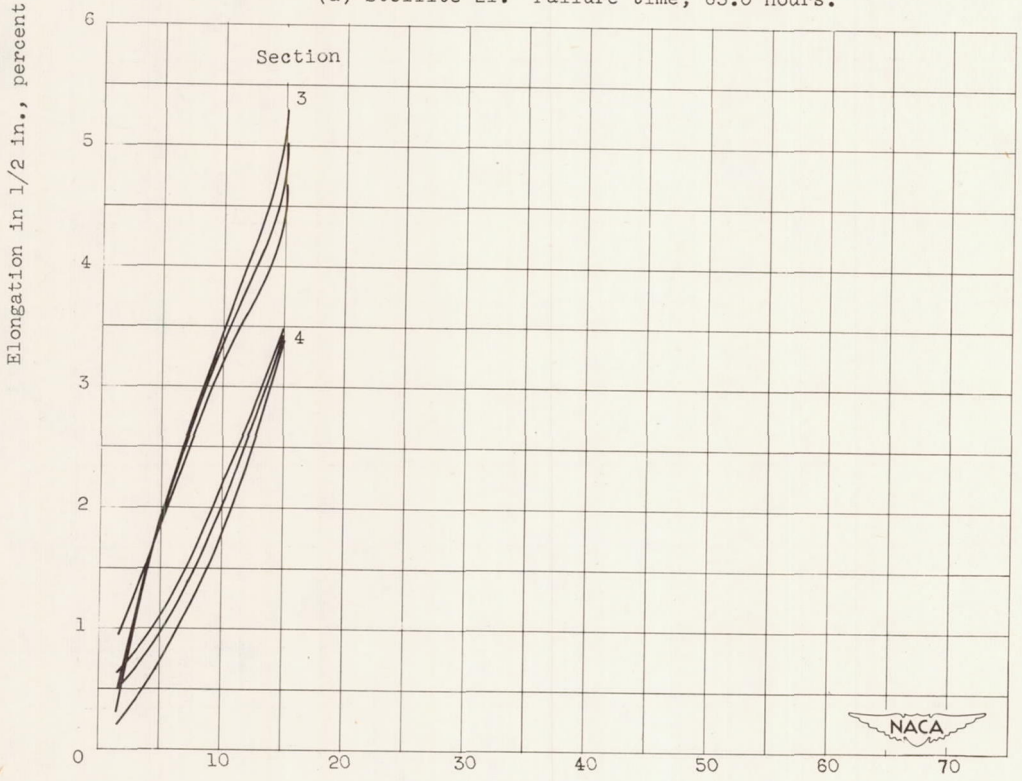


Figure 6. - Elongation distribution in Hastelloy B blade after 15 hours of operation.

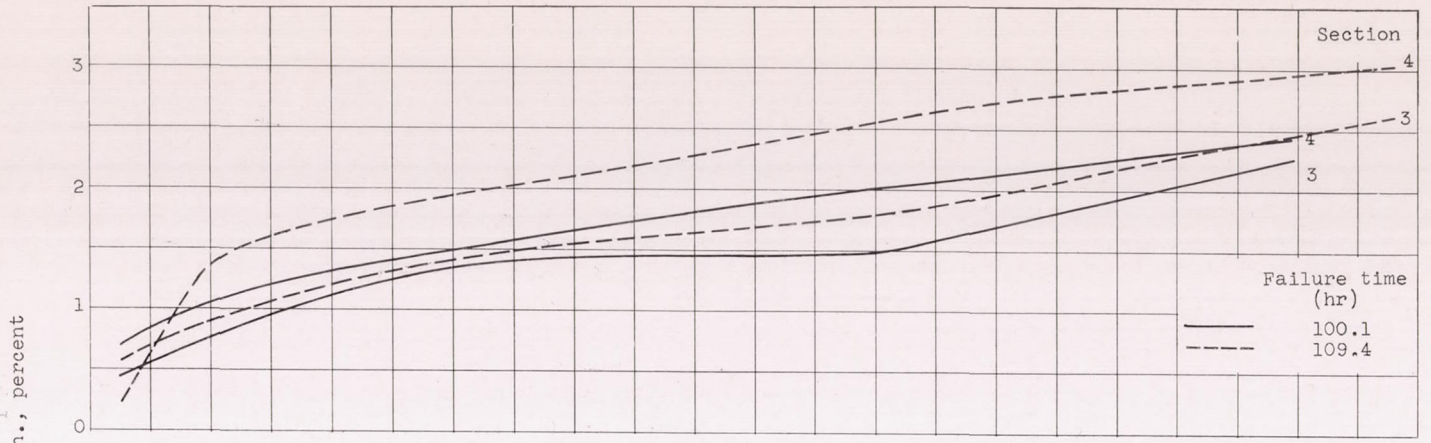


(a) Stellite 21. Failure time, 63.0 hours.

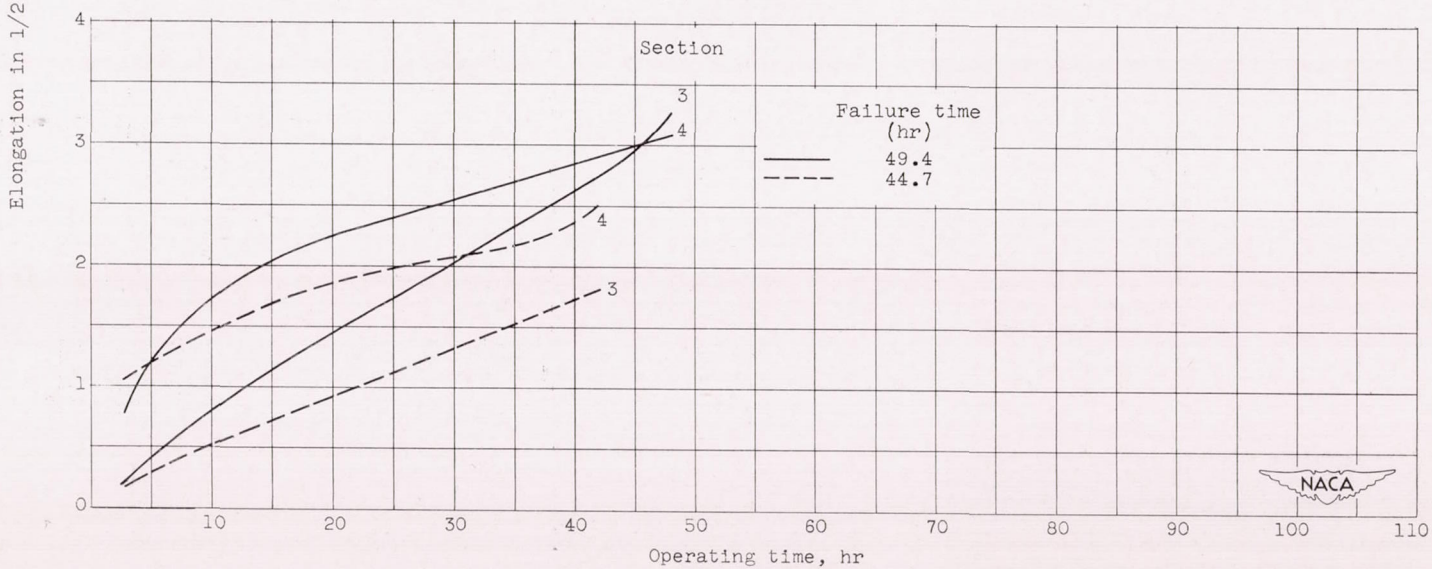


(b) Hastelloy B. Failure time, 15.0 hours.

Figure 7. - Creep curves during engine operation for blades that had true failures.



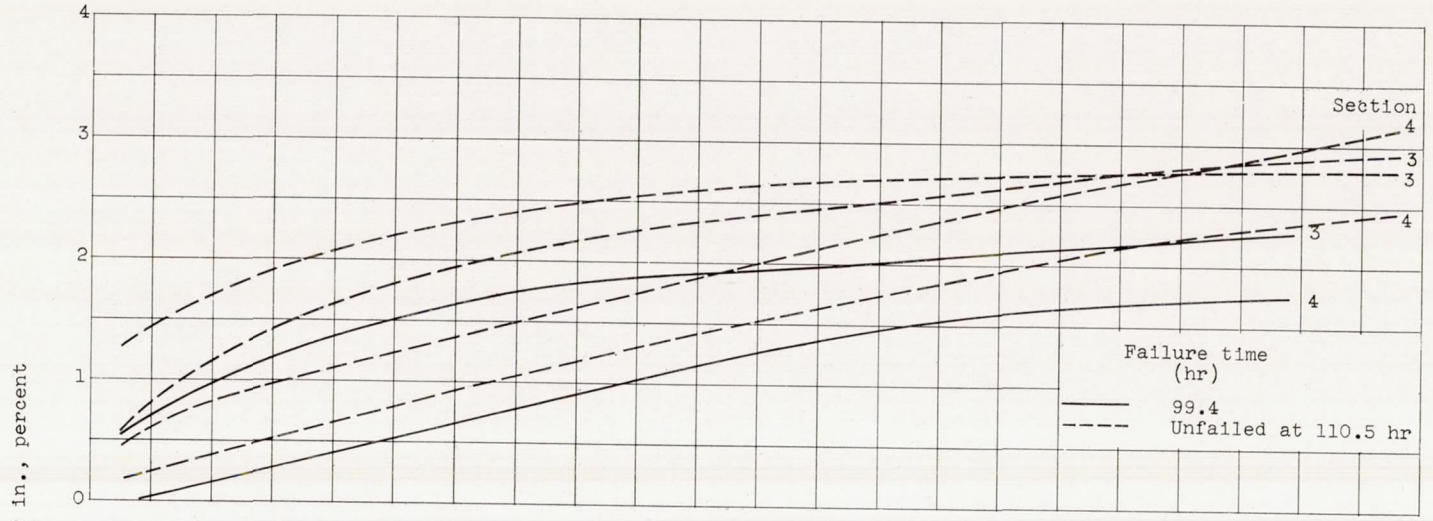
(c) Cast S-816.



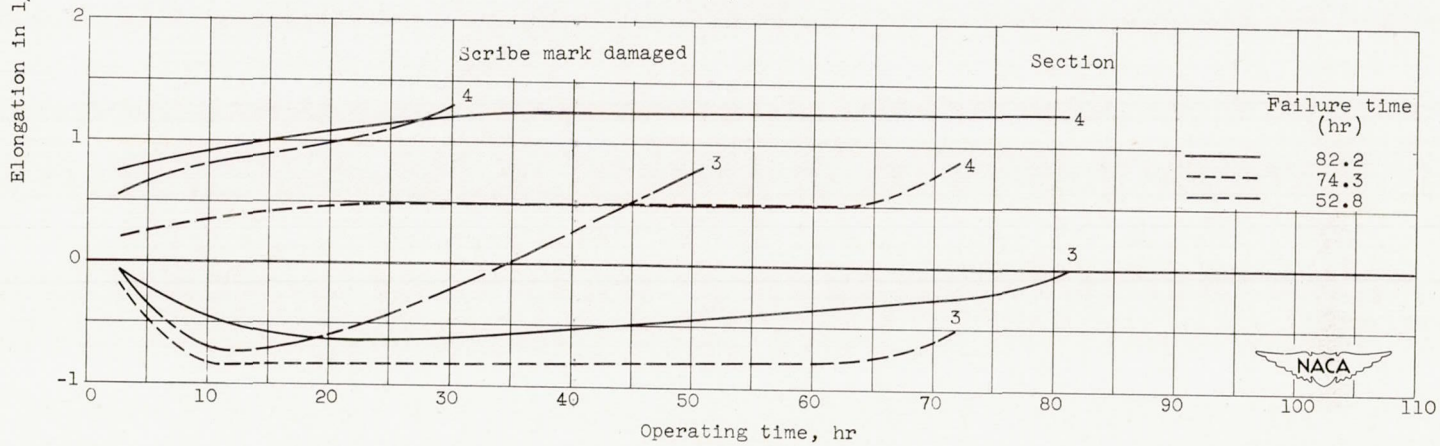
Elongation in 1/2 in., percent

(d) Forged S-816.

Figure 7. - Continued. Creep curves during engine operation for blades that had true failures.

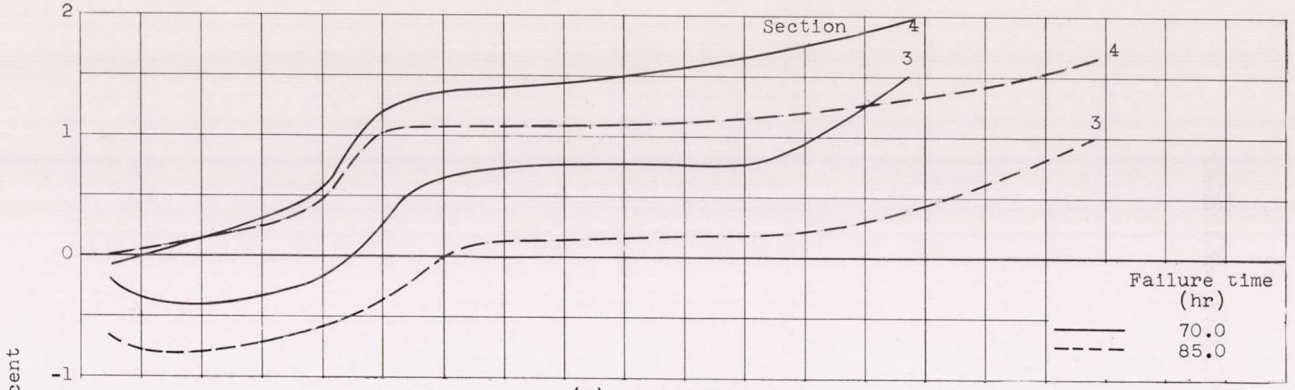


(e) X-40.

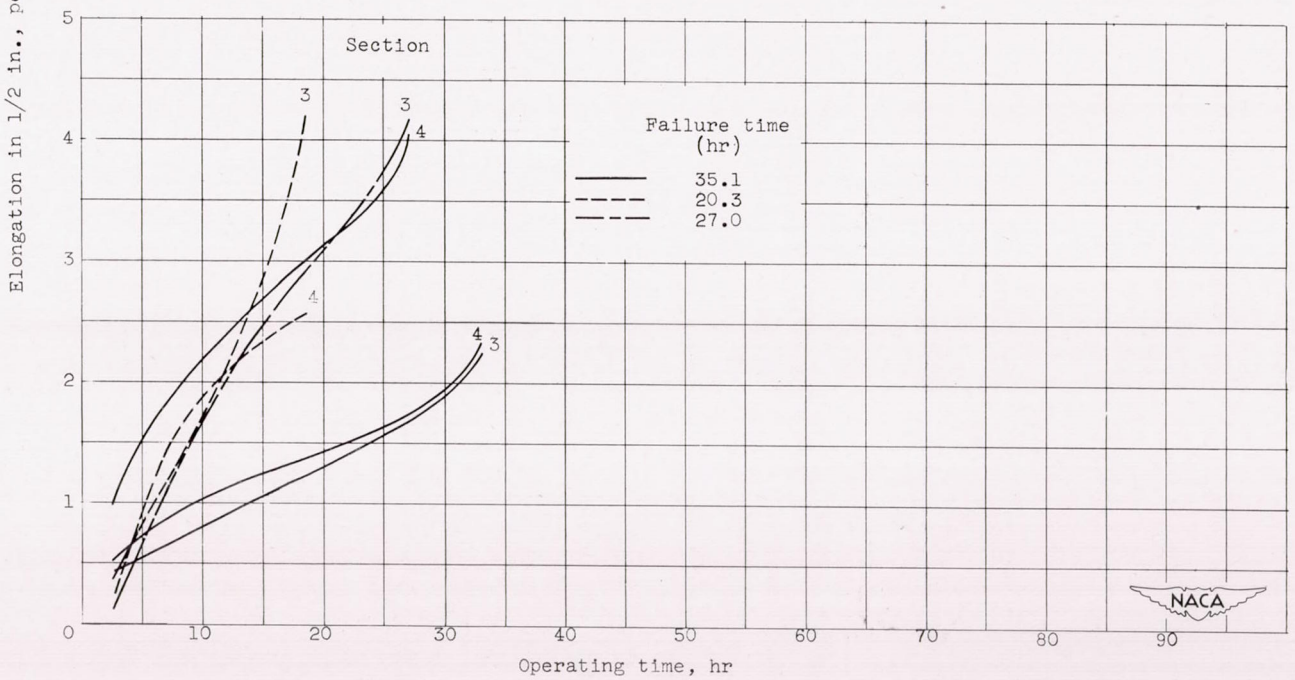


(f) Nimonic 80.

Figure 7. - Continued. Creep curves during engine operation for blades that had true failures.

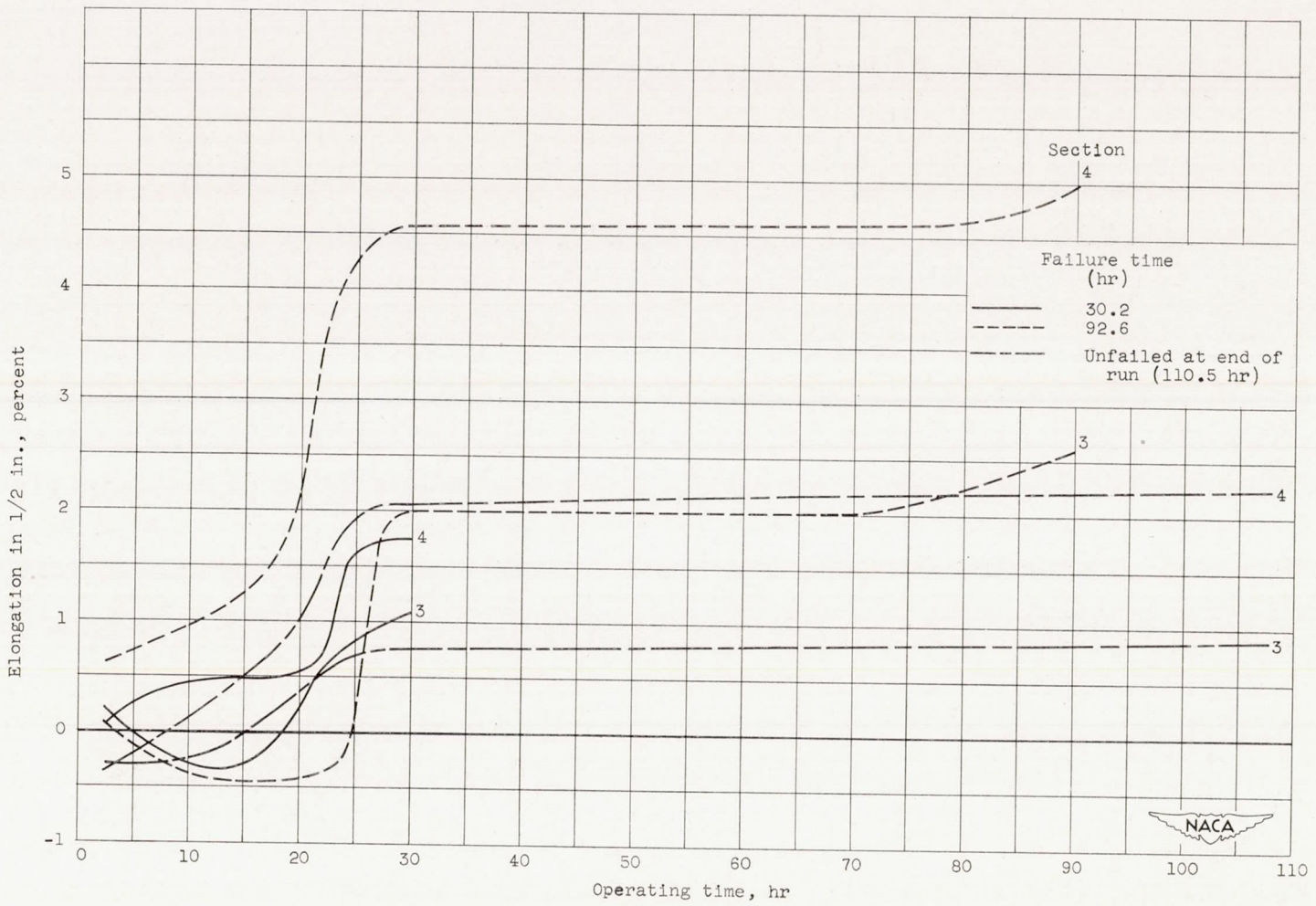


(g) Refractaloy 26.



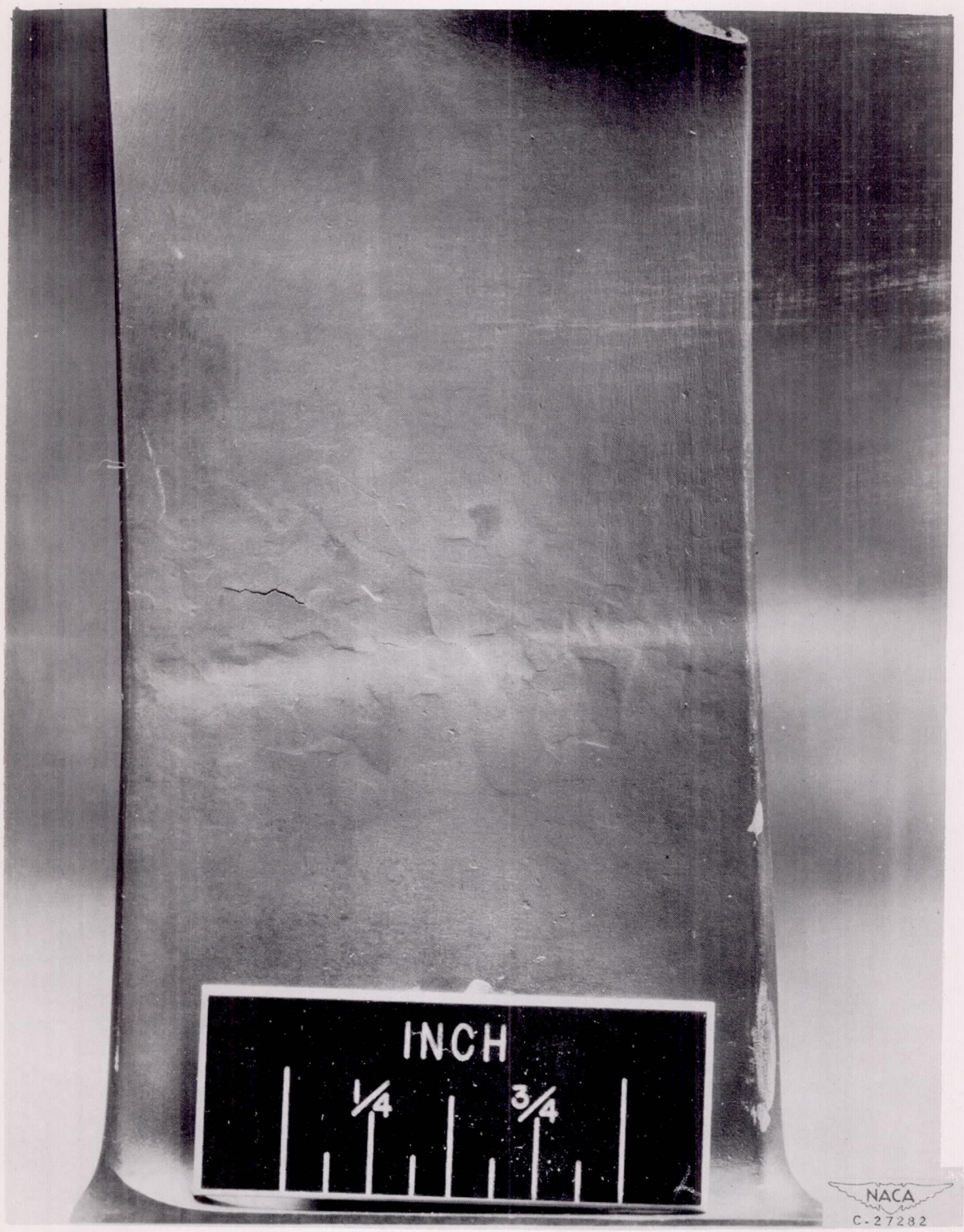
(h) N-155.

Figure 7. - Continued. Creep curves during engine operation for blades that had true failures.



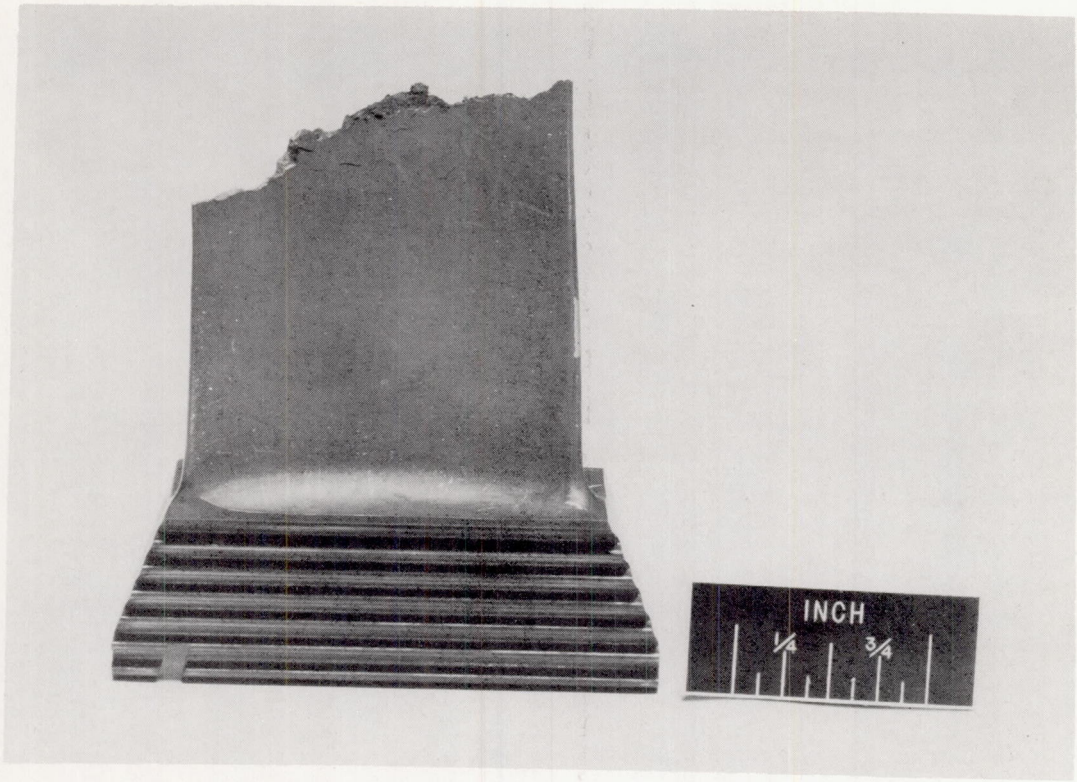
(i) Inconel X.

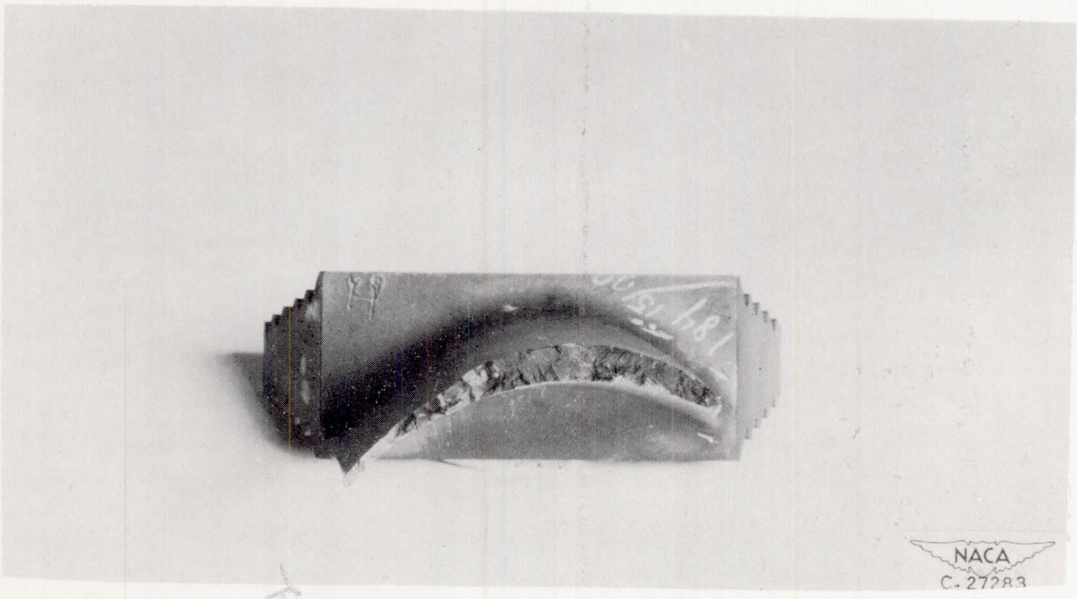
Figure 7. - Concluded. Creep curves during engine operation for blades that had true failures.



(a) Surface distraction and beginning of failure after 45 hours of operation.

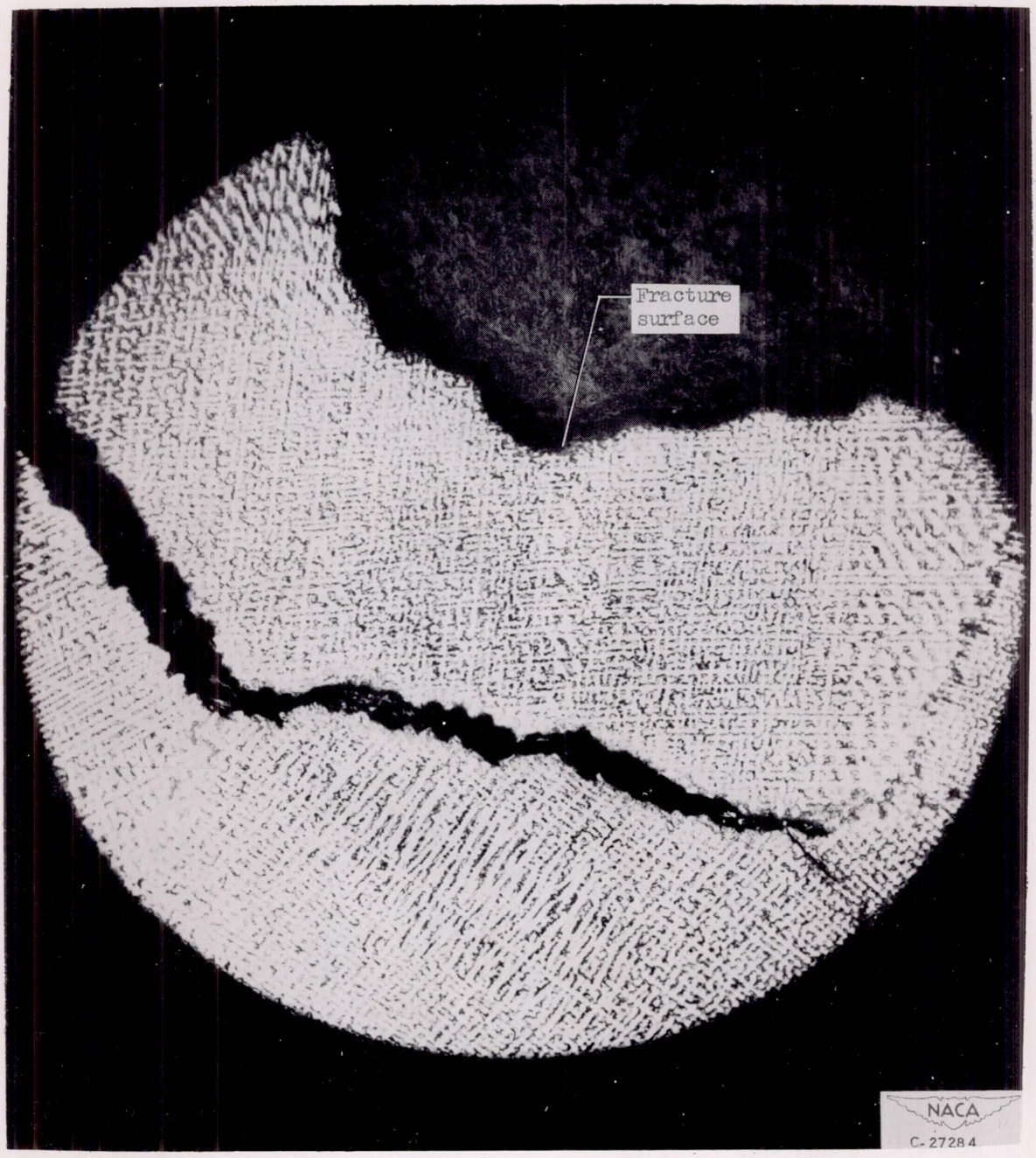
Figure 8. - Results of metallurgical examination of Stellite 21 blade.





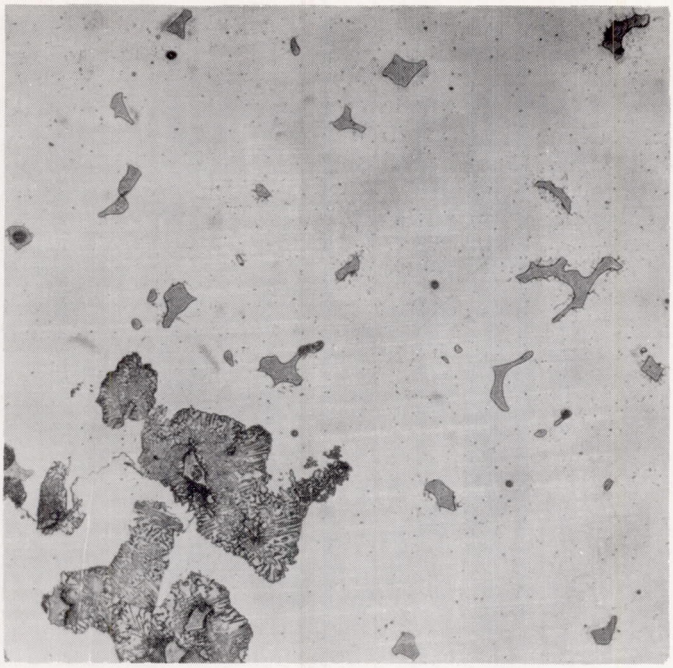
(b) Fractured blade after 46.2 hours of operation. Fracture is typical of sample failure.

Figure 8. - Continued. Results of metallurgical examination of Stellite 21 blade.

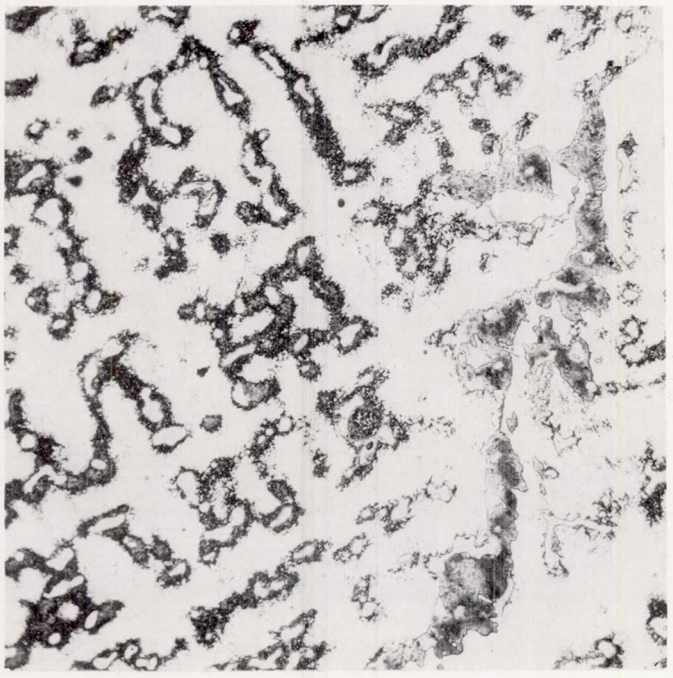


(c) Intergranular fracture surface and crack. Electrolytically etched in 10-percent chromic acid. X50.

Figure 8. - Continued. Results of metallurgical examination of Stellite 21 blade.

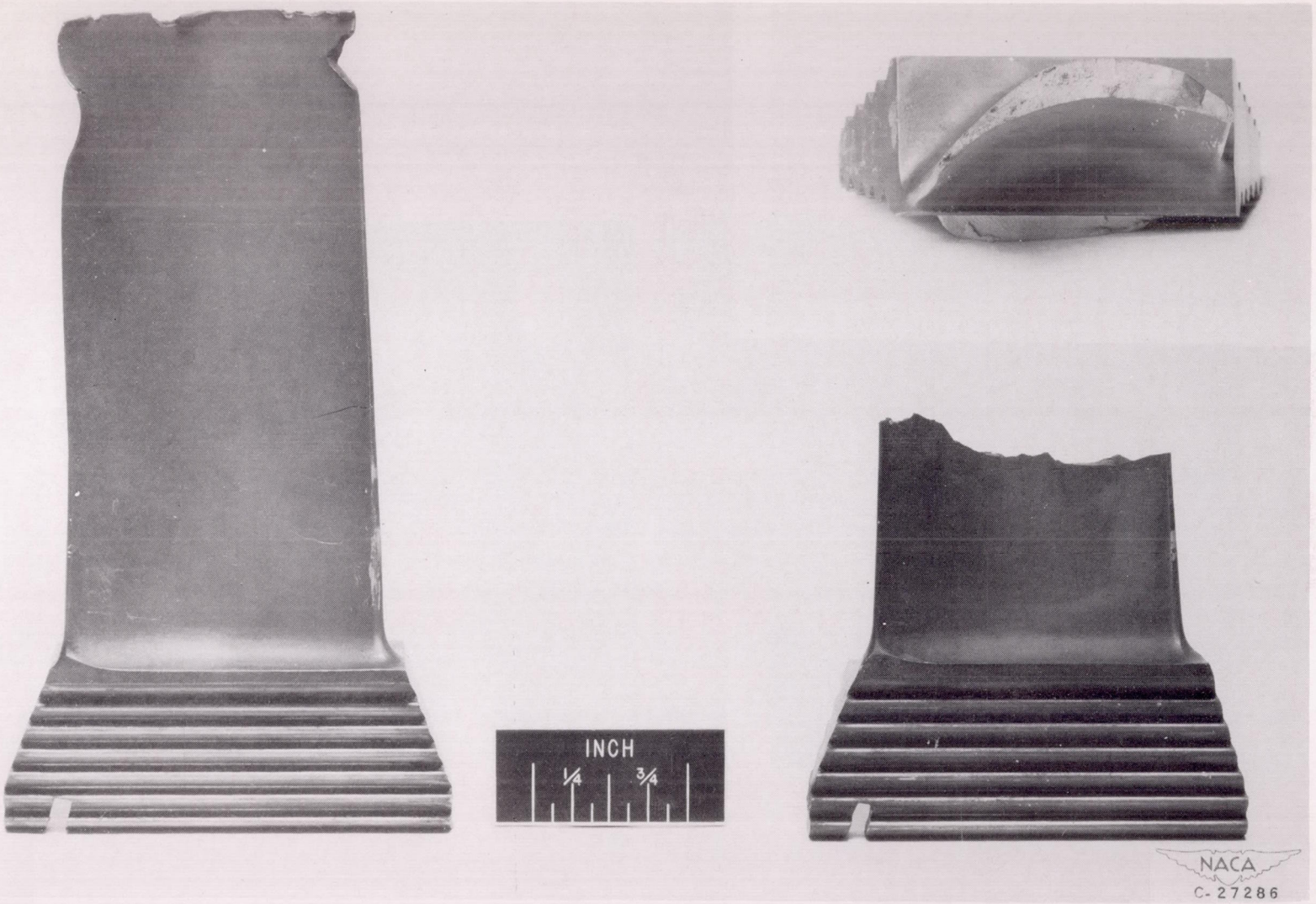


(d) Structure before operation. Electrolytically etched in 10-percent chromic acid. X250.



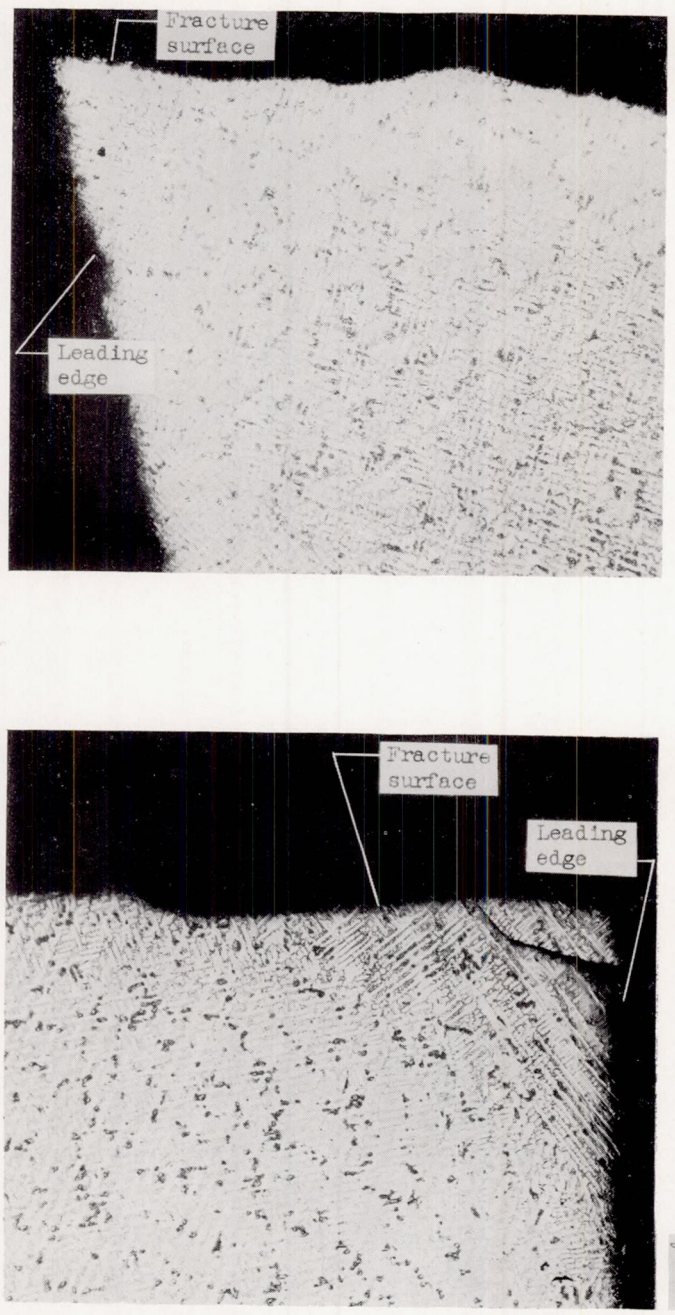
(e) Structure after operation. Electrolytically etched in 10-percent chromic acid. X250.

Figure 8. - Concluded. Results of metallurgical examination of Stellite 21 blade.



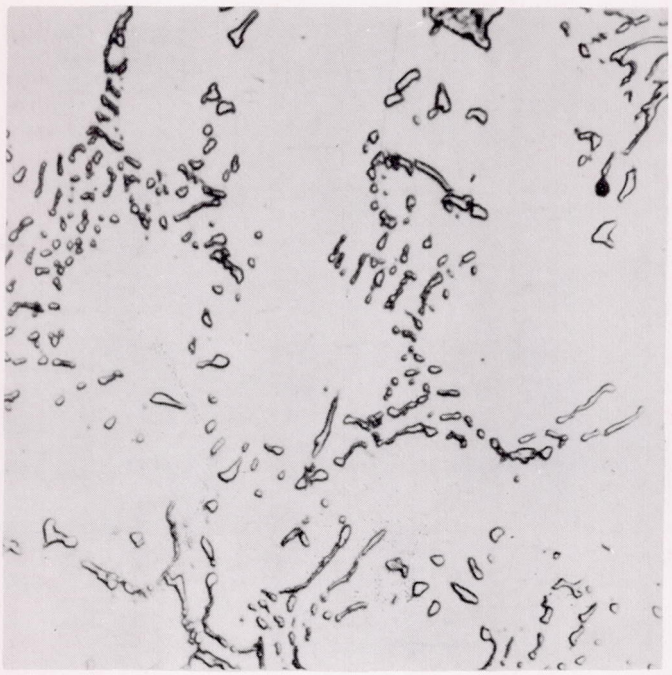
(a) Typical blade failure.

Figure 9. - Results of metallurgical examination of cast S-816.

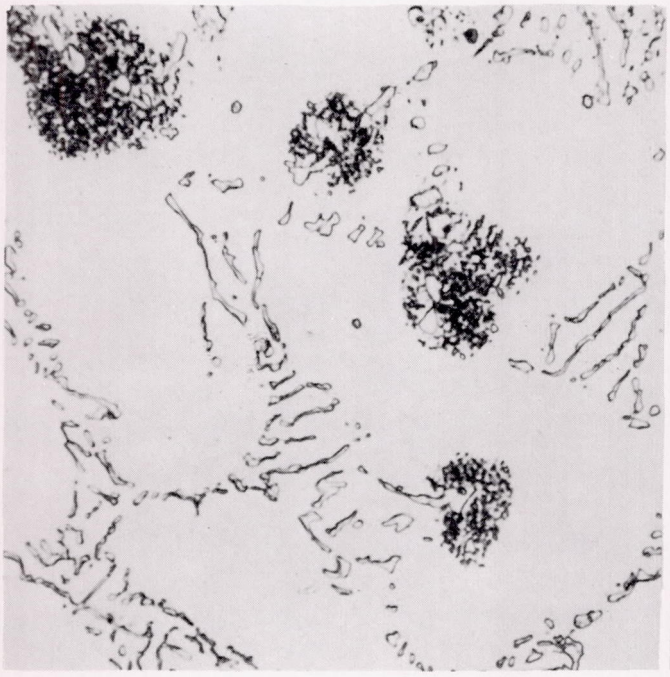


(b) Transcrystalline fracture at leading edges. Electrolytically etched in 10-percent chromic acid; X50.

Figure 9. - Continued. Results of metallurgical examination of cast S-816 blade.

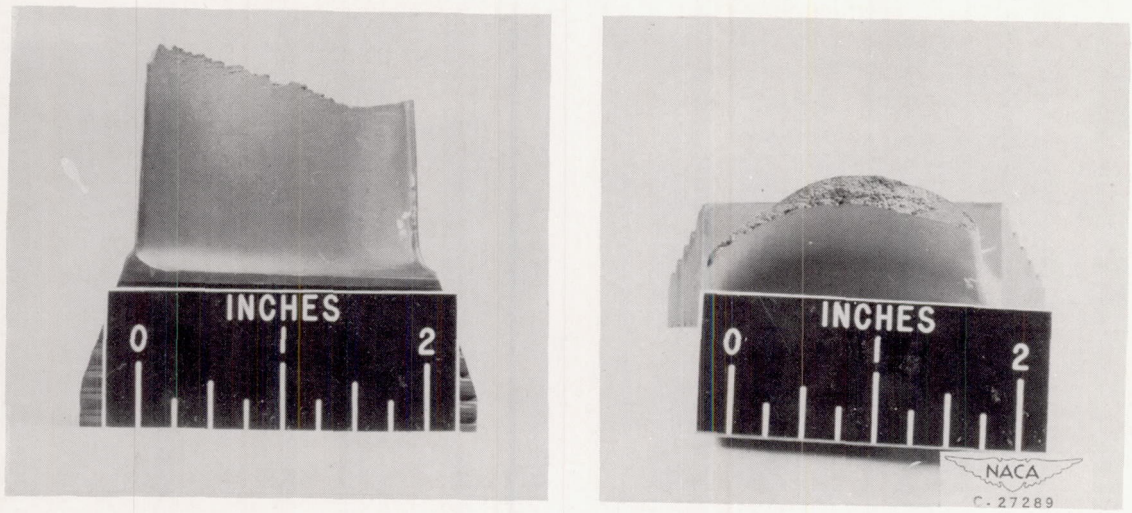


(c) Structure before operation. Electrolytically etched in 10-percent chromic acid, X1000.



(d) Structure after operation. Electrolytically etched in 10-percent chromic acid, X1000.

Figure 9. - Concluded. Results of metallurgical examination of cast S-816 blade.



(a) Typical blade failure.

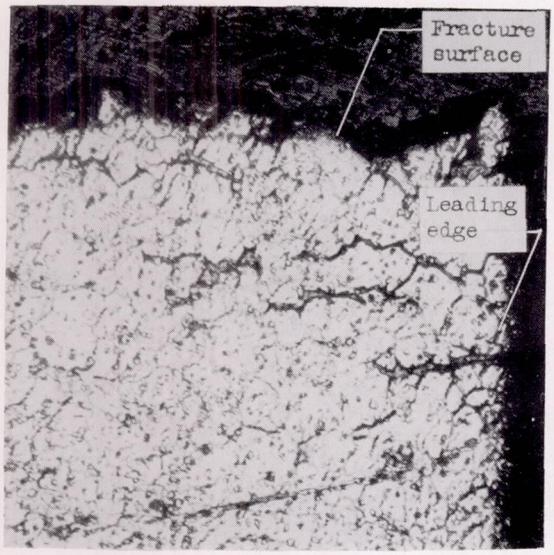


Center of blade, A.S.T.M. 4 to 6

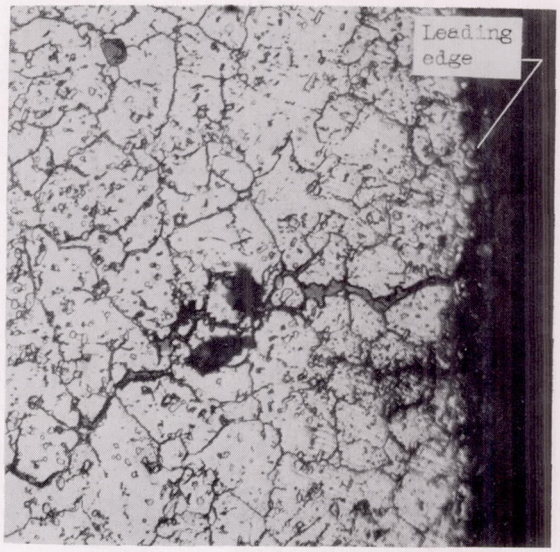
Leading edge of blade (zone of failure origin), A.S.T.M. 6 to 7

(b) Grain size. Electrolytically etched in 10-percent chromic acid, X100.

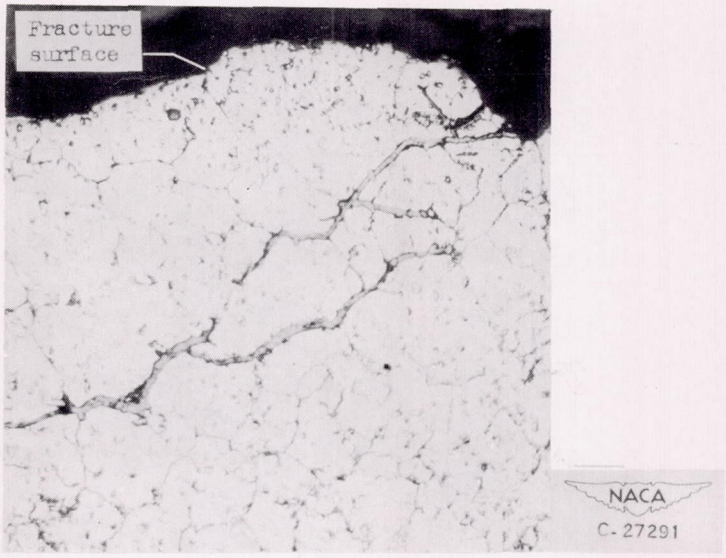
Figure 10. - Results of metallurgical examination of forged S-816 blade.



Intercrystalline cracking and fracture path at leading edge; X150.



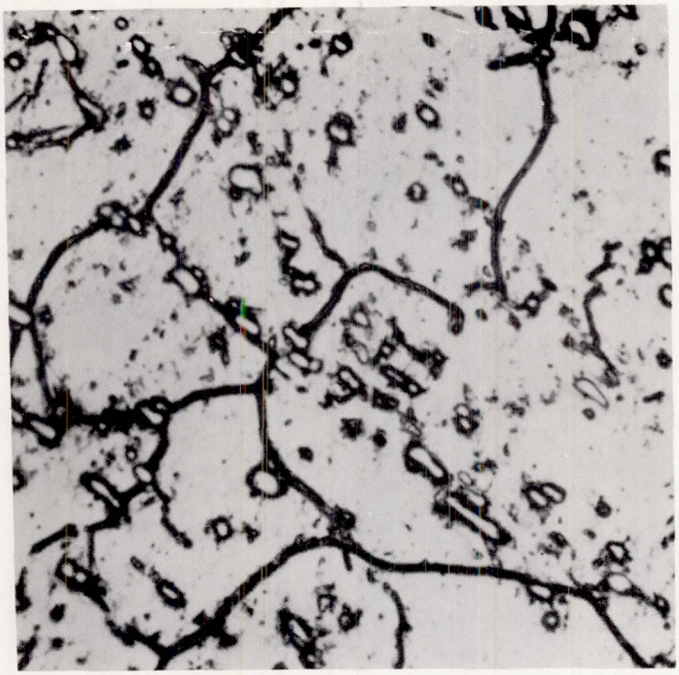
Intercrystalline crack at leading edge; X250.



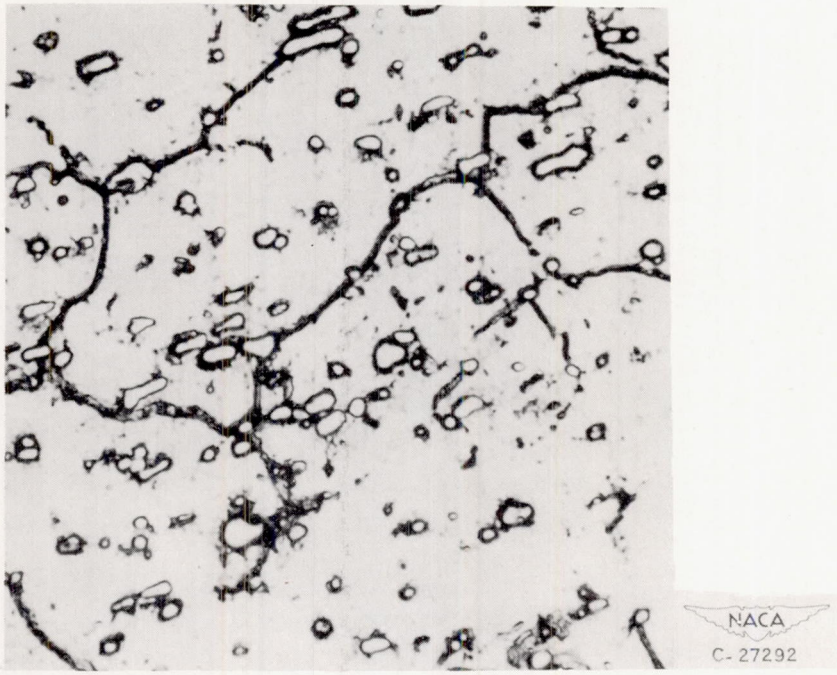
Transcrystalline fatigue fracture path nucleated by intercrystalline cracks; X250.

(c) Nature of fracture propagation. Electrolytically etched in 10-percent chromic acid.

Figure 10. - Continued. Results of metallurgical examination of forged S-816 blade.

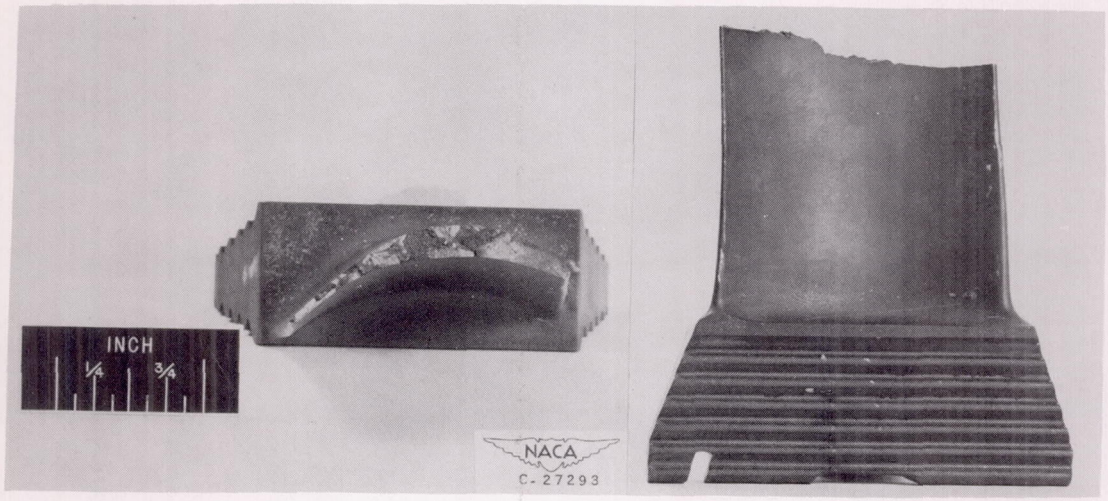


(d) Structure before operation. Electrolytically etched in 10-percent chromic acid; X1000.

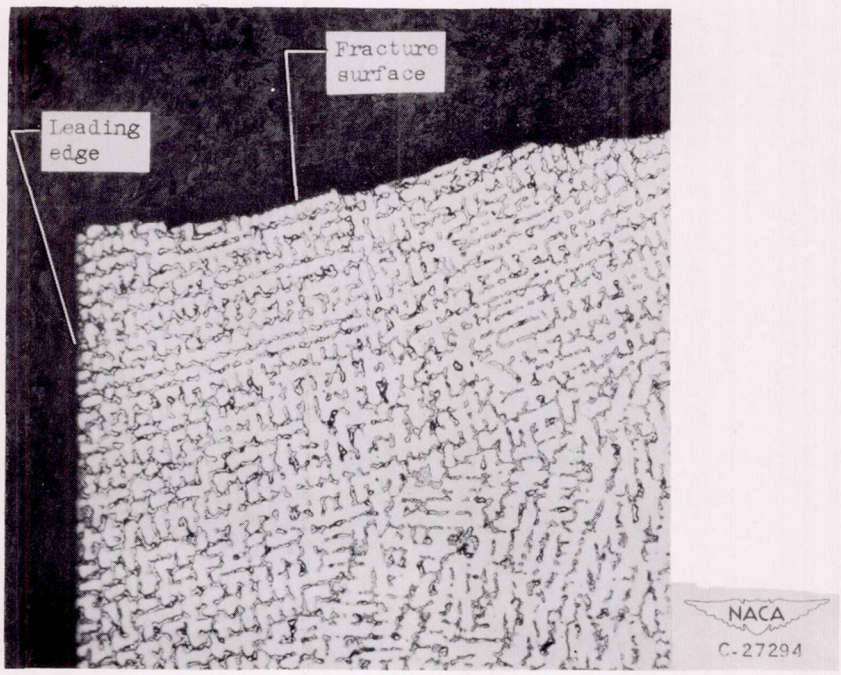


(e) Structure after operation. Electrolytically etched in 10-percent chromic acid; X1000.

Figure 10. - Concluded. Results of metallurgical examination of forged S-816 blade.

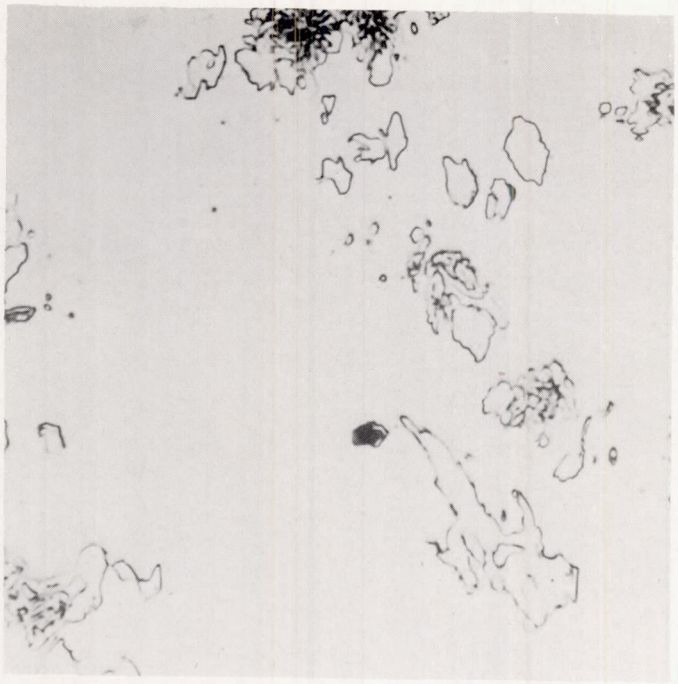


(a) Initial true blade failure after 99.4 hours of operation. Remaining blades did not fail.

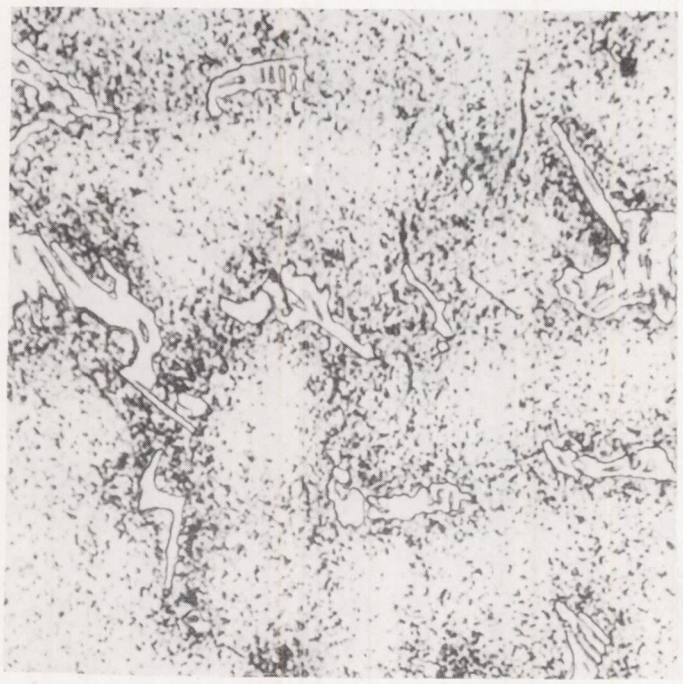


(b) Transcrystalline fracture path at leading edge. Electrolytically etched in 10-percent chromic acid; X100.

Figure 11. - Results of metallurgical examination of X-40 blades.

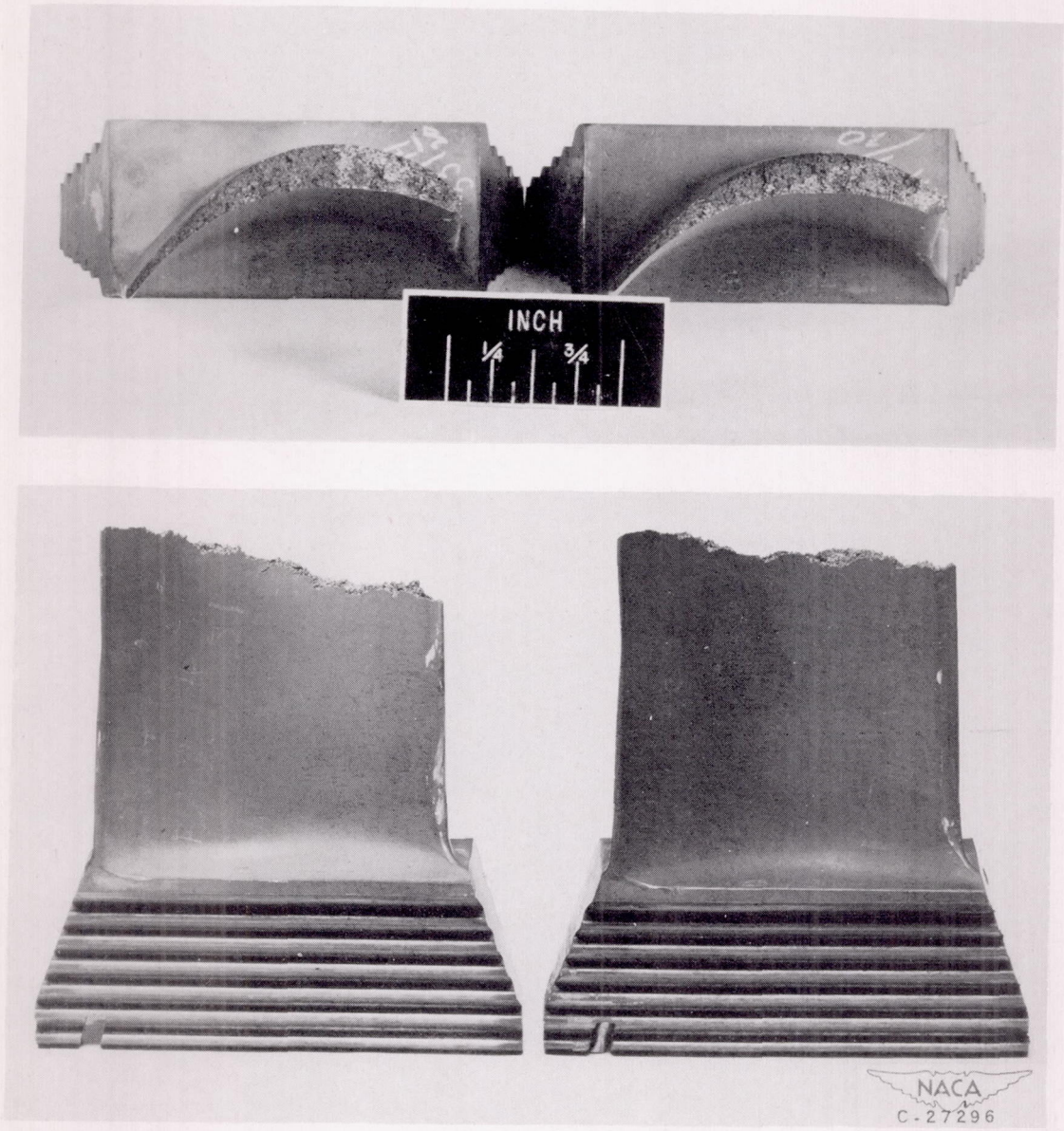


(c) Structure before operation. Electrolytically etched in 10-percent chromic acid; X1000.



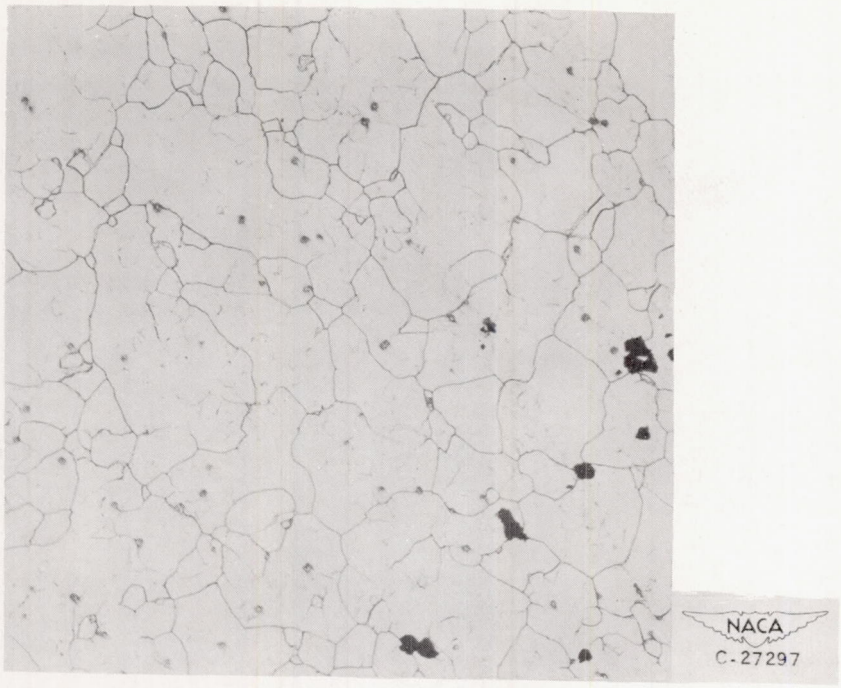
(d) Structure after operation. Electrolytically etched in 10-percent chromic acid; X1000.

Figure 11. - Concluded. Results of metallurgical examination of X-40 blades.

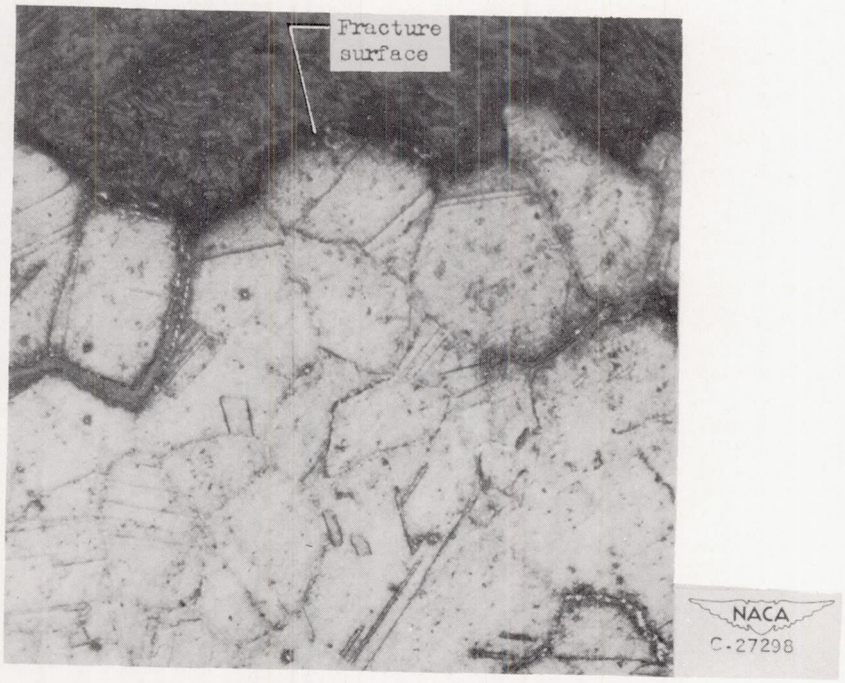


(a) Typical blades failure.

Figure 12. - Results of metallurgical examination of Nimonic 80 blades.

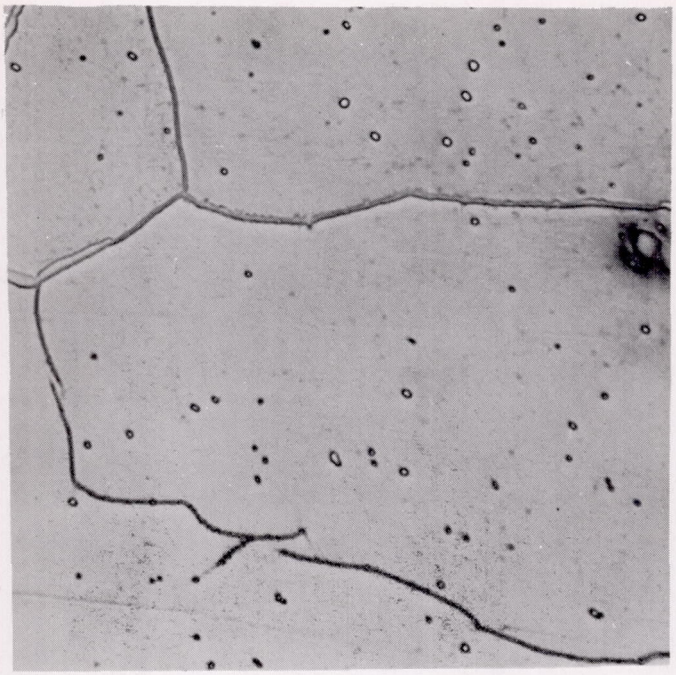


(b) Grain size throughout blade, A.S.T.M. 2 to 4. Electrolytically etched in 10-percent chromic acid; X100.

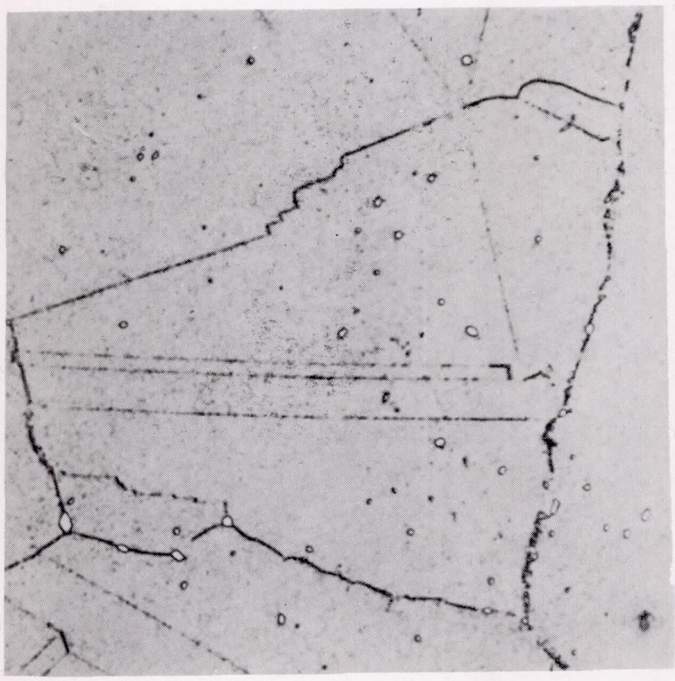


(c) Nature of fracture propagation. Electrolytically etched in 10-percent chromic acid; X150, oblique illumination.

Figure 12. - Continued. Results of metallurgical examination of Nimonic 80 blades.

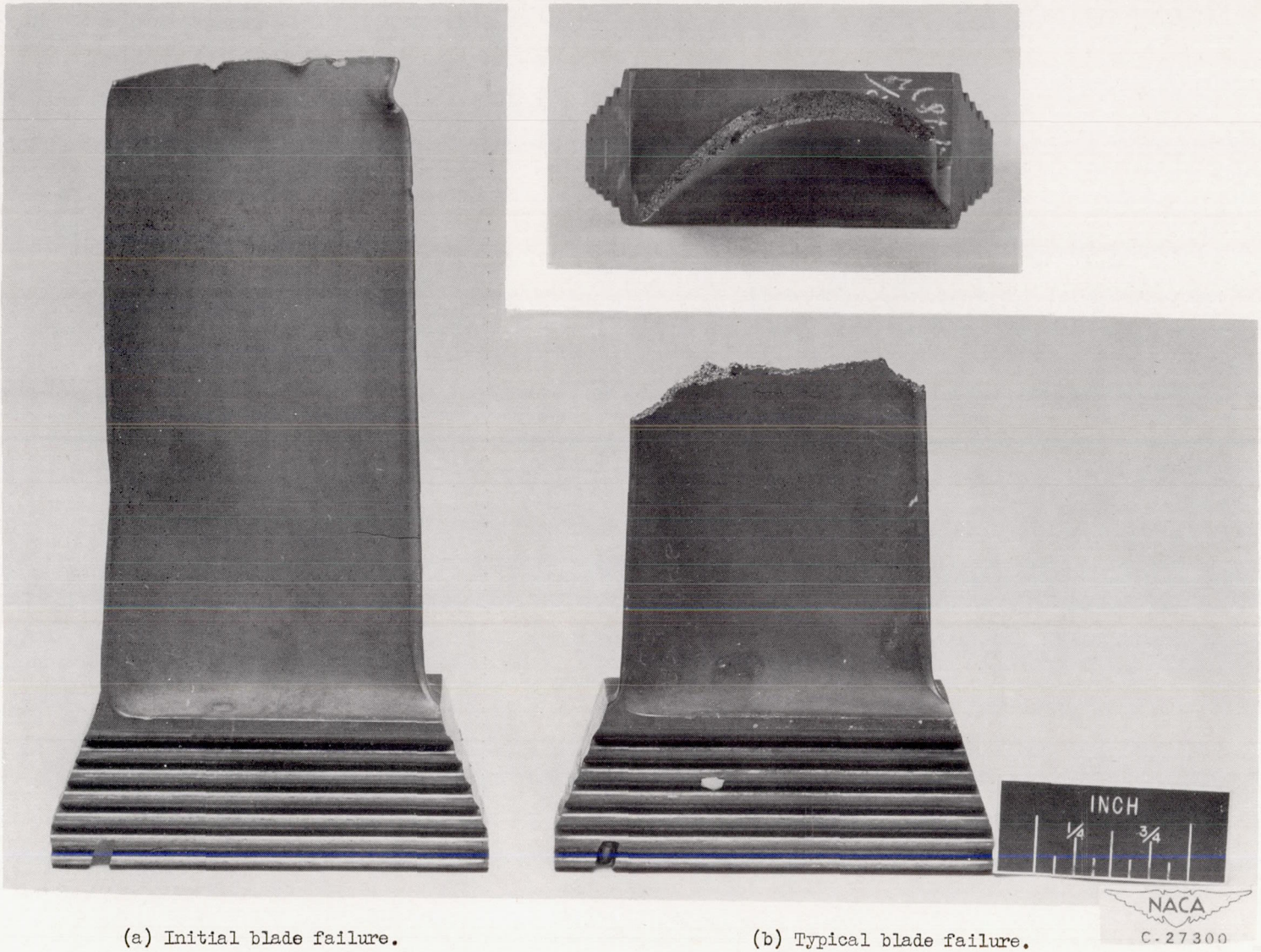


(d) Structure before engine operation. Electrolytically etched in 10-percent chromic acid; X1000



(e) Structure after engine operation. Electrolytically etched in 10-percent chromic acid: X1000.

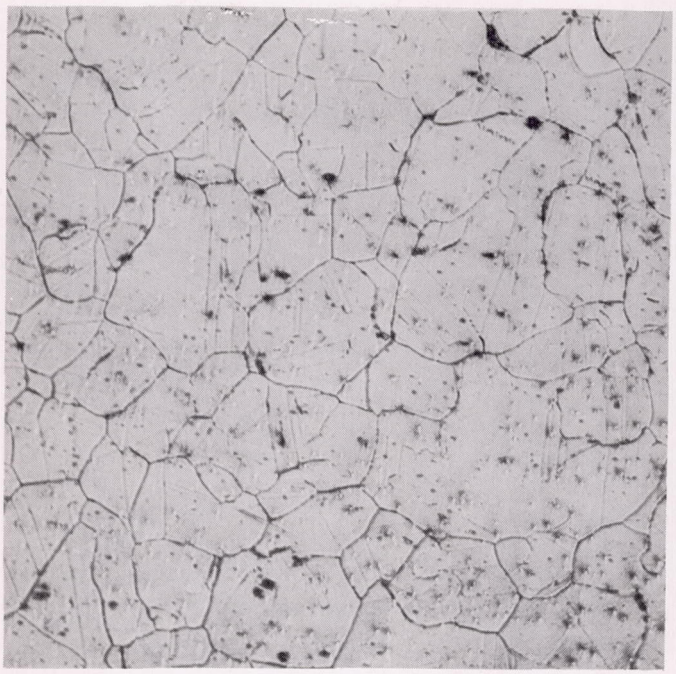
Figure 12. - Concluded. Results of metallurgical examination of Nimonic 80 blades.



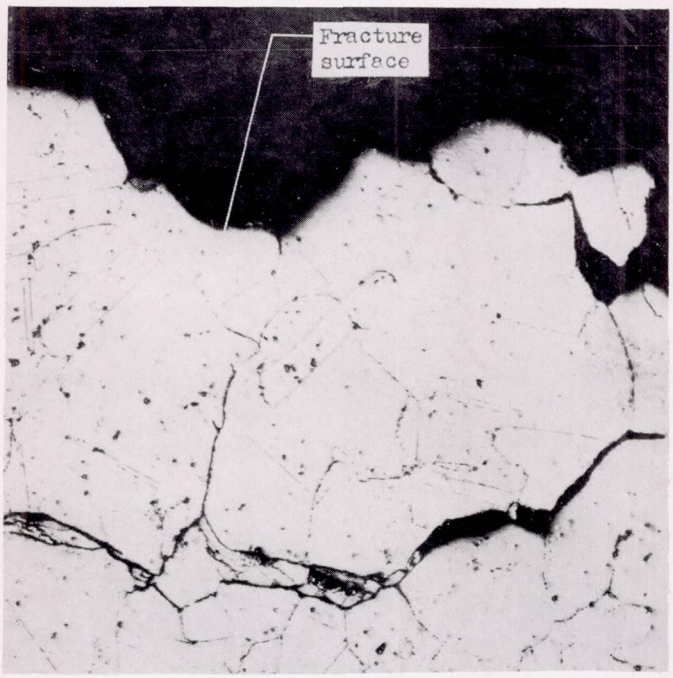
(a) Initial blade failure.

(b) Typical blade failure.

Figure 13. - Results of metallurgical examination of Refractaloy 26 blades.

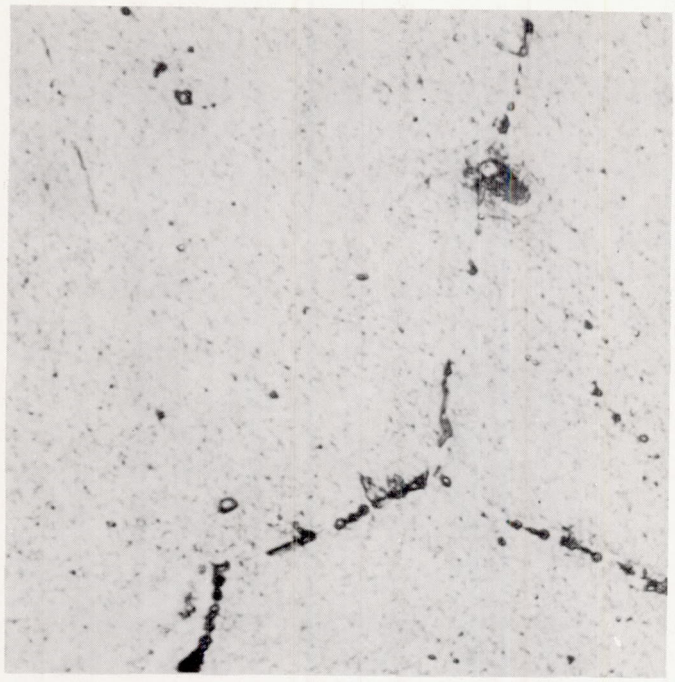


(c) Grain size throughout blade, A.S.T.M. 2 to 3. Electrolytically etched in 10-percent chromic acid; X100; oblique illumination.

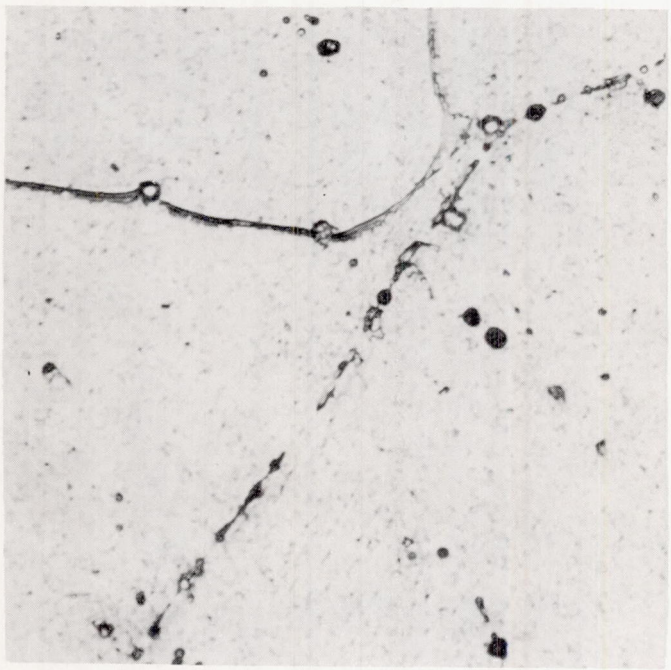


(d) Nature of fracture propagation. Electrolytically etched in 10-percent chromic acid; X150.

Figure 13. - Continued. Results of metallurgical examination of Refractaloy 26 blades.

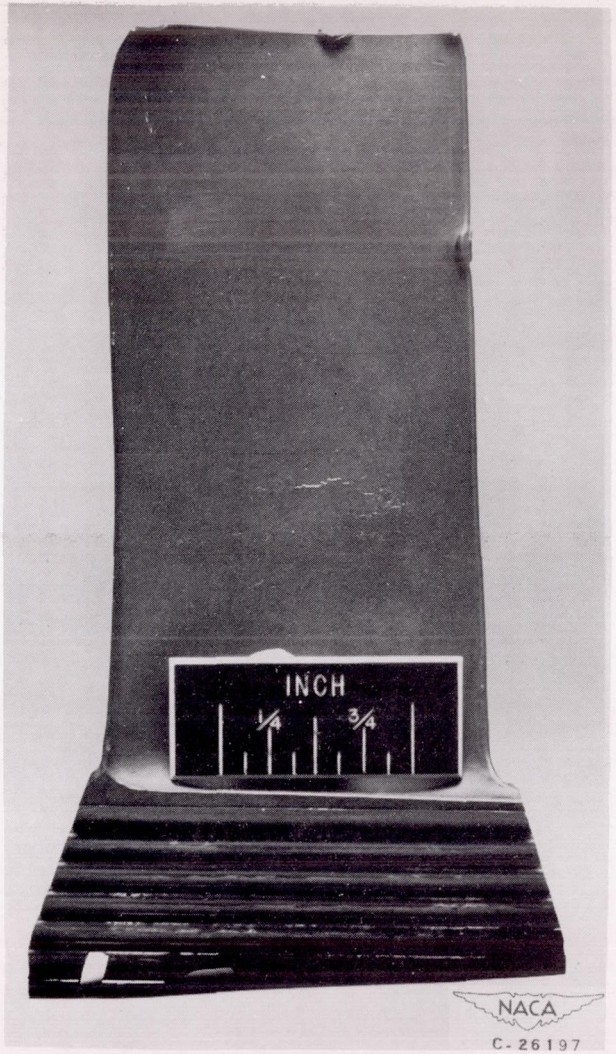


(e) Structure before operation. Electrolytically etched in 10-percent chromic acid; X1000.

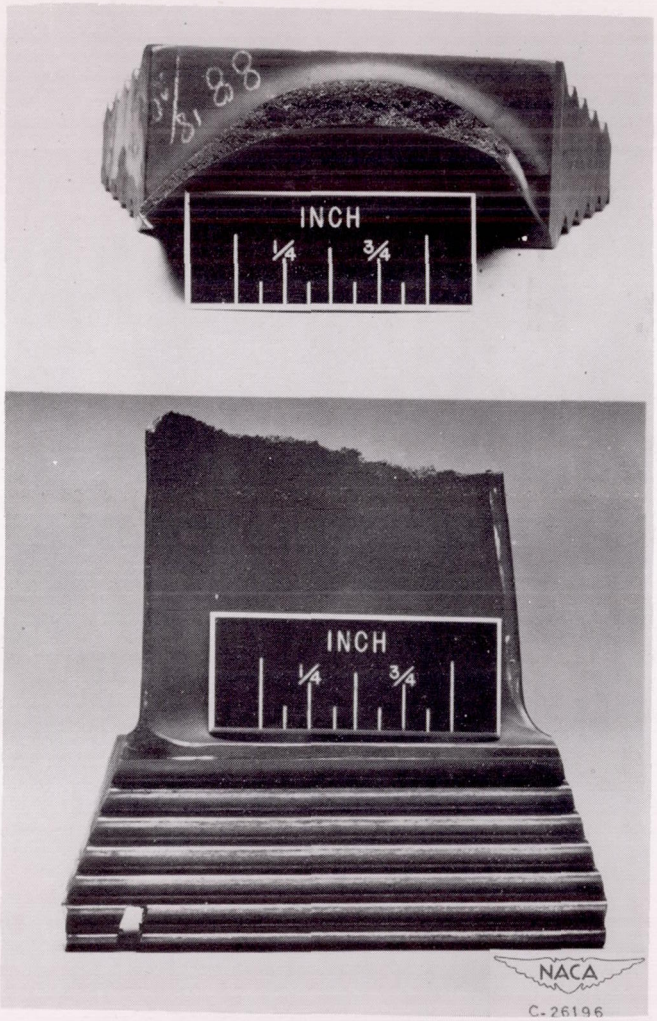


(f) Structure after operation. Electrolytically etched in 10-percent chromic acid; X1000.

Figure 13. - Concluded. Results of metallurgical examination of Refractaloy 26 blades.

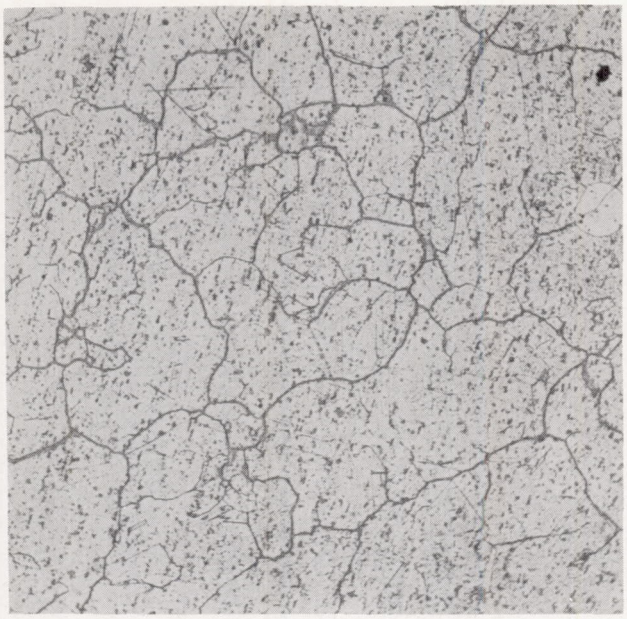


(a) Beginning of failure.

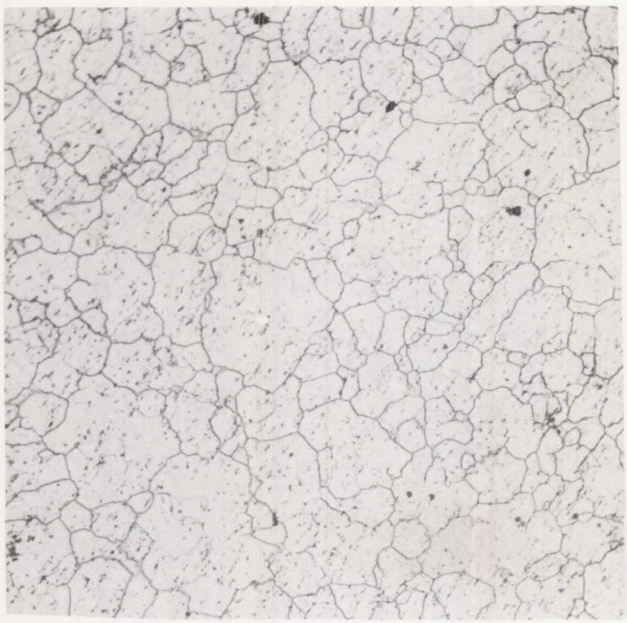


(b) Typical failure.

Figure 14. - Results of metallurgical examination of N-155 blades.



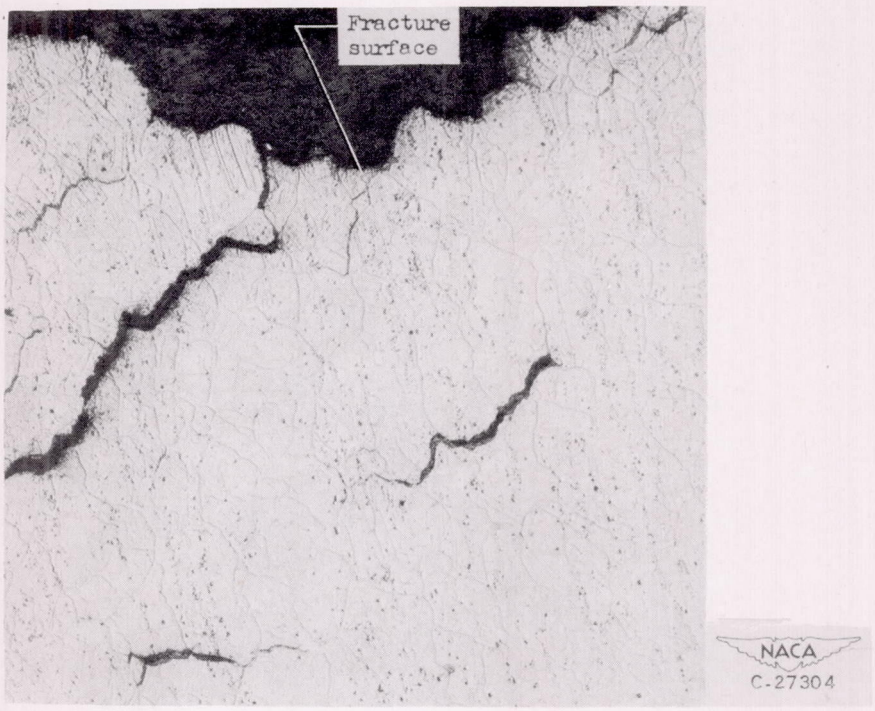
Center of blade, A.S.T.M. 2 to 4.



Edges of blade, A.S.T.M. 3 to 5.

(c) Grain size. Electrolytically etched in 10-percent chromic acid; X100.

Figure 14. - Continued. Results of metallurgical examination of N-155 blades.

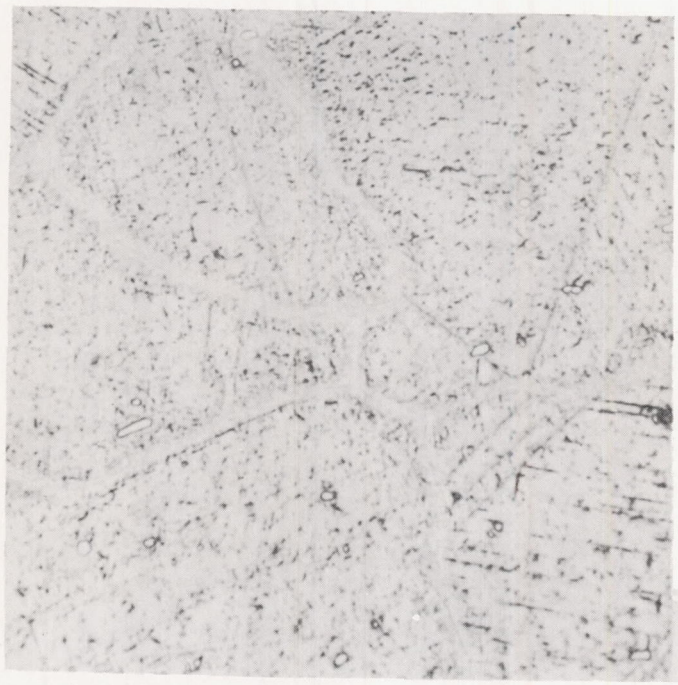


(d) Intercrystalline fracture and cracking. Electrolytically etched in 10-percent chromic acid; X100.

Figure 14. - Continued. Results of metallurgical examination of N-155 blades.

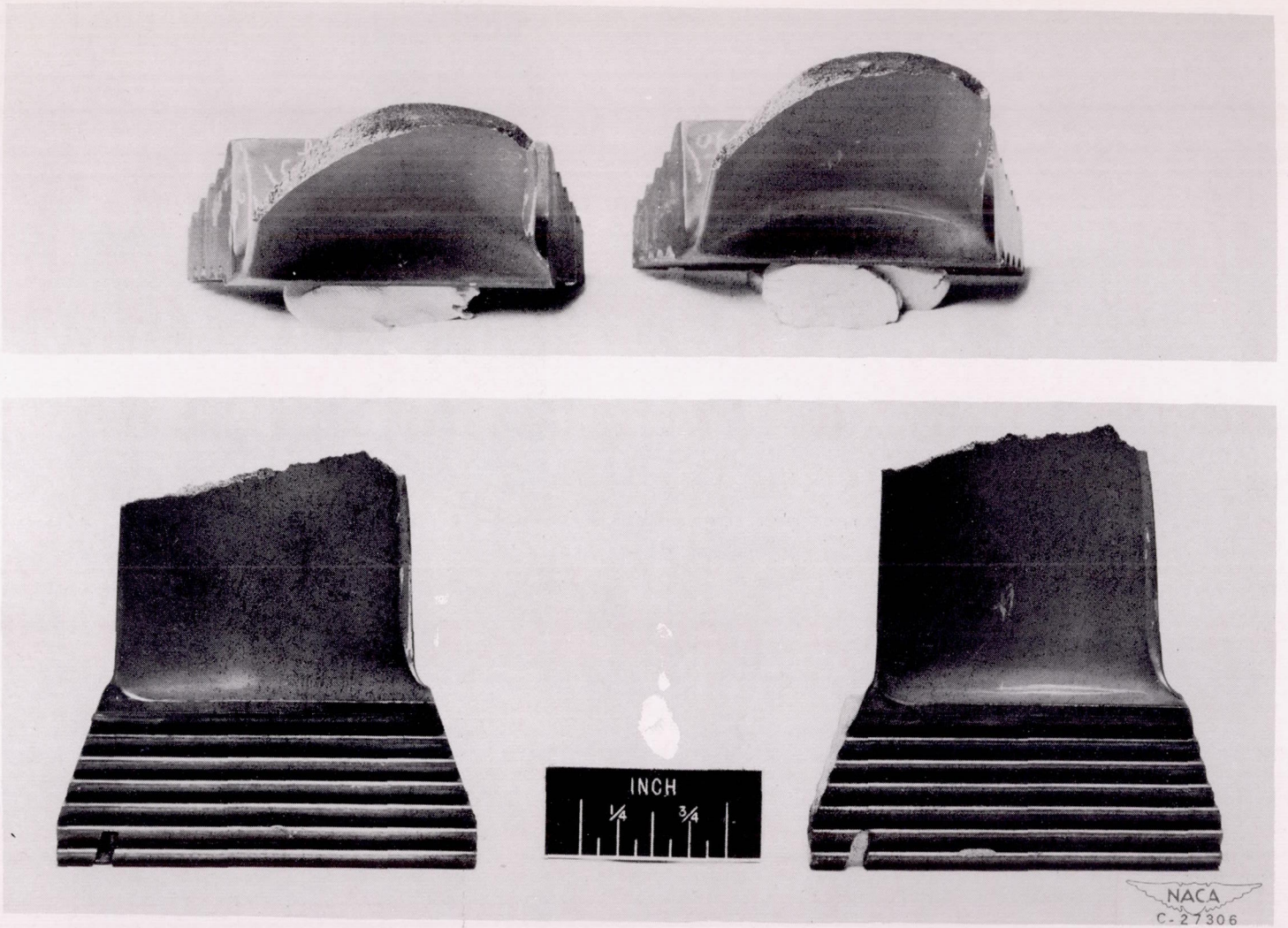


(e) Structure before operation. Electrolytically etched in 10-percent chromic acid; X100.



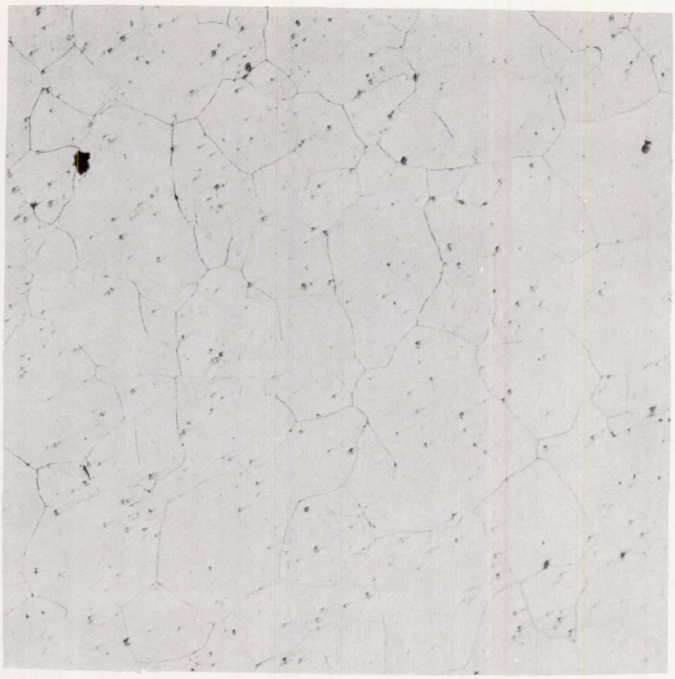
(f) Structure after operation. Electrolytically etched in 10-percent chromic acid; X1000.

Figure 14. - Concluded. Results of metallurgical examination of N-155 blades.

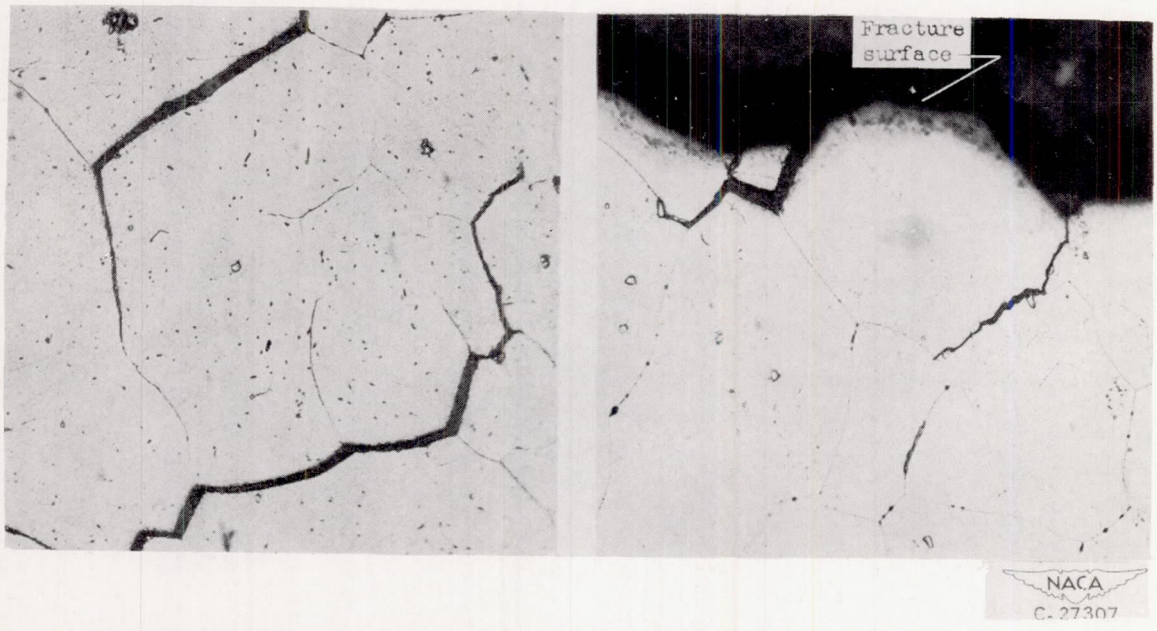


(a) Typical blade failure.

Figure 15. - Results of metallurgical examination of Inconel X.

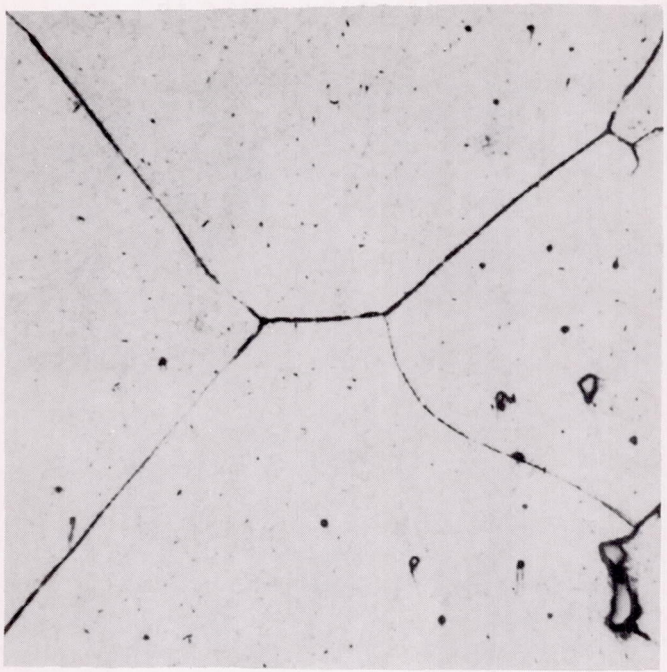


(b) Grain size throughout blades, A.S.T.M. 2 to 3. Electrolytically etched in 10-percent chromic acid; X100.

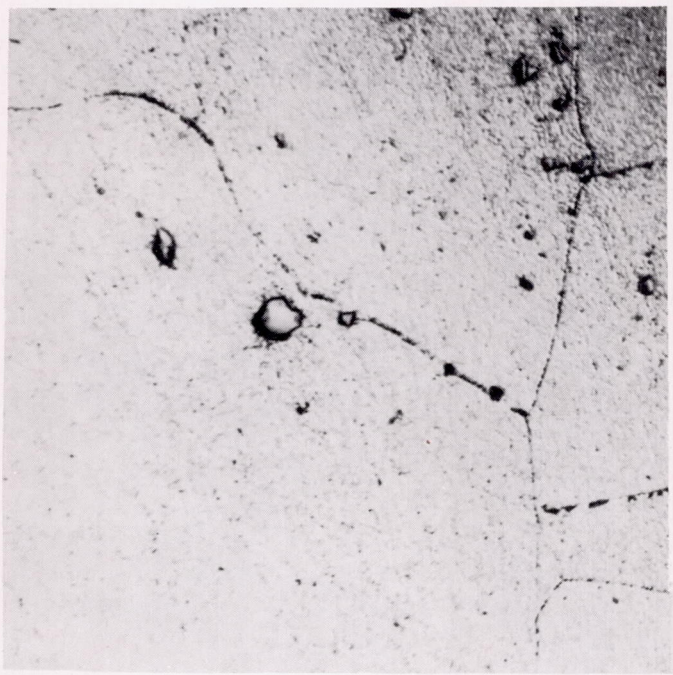


(c) Intercrystalline fracture and cracking. Electrolytically etched in 10-percent chromic acid; X250.

Figure 15. - Continued. Results of metallurgical examination of Inconel X.



(d) Structure before operation. Electrolytically etched in 10-percent chromic acid; X1000.



(e) Structure after operation. Electrolytically etched in chromic acid. X1000.

Figure 15. - Concluded. Results of metallurgical examination of Inconel X.

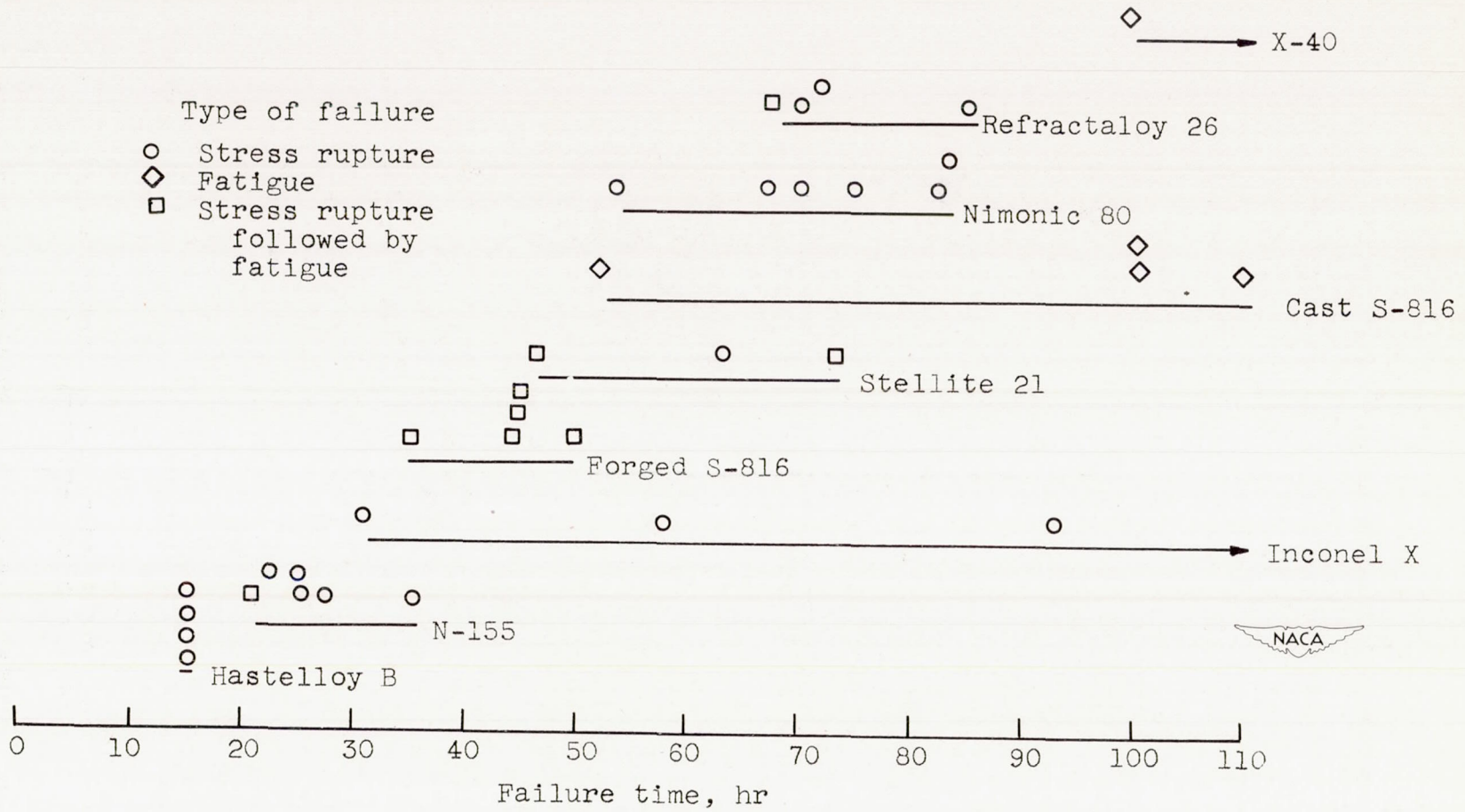


Figure 16. - Classification of true blade failures.

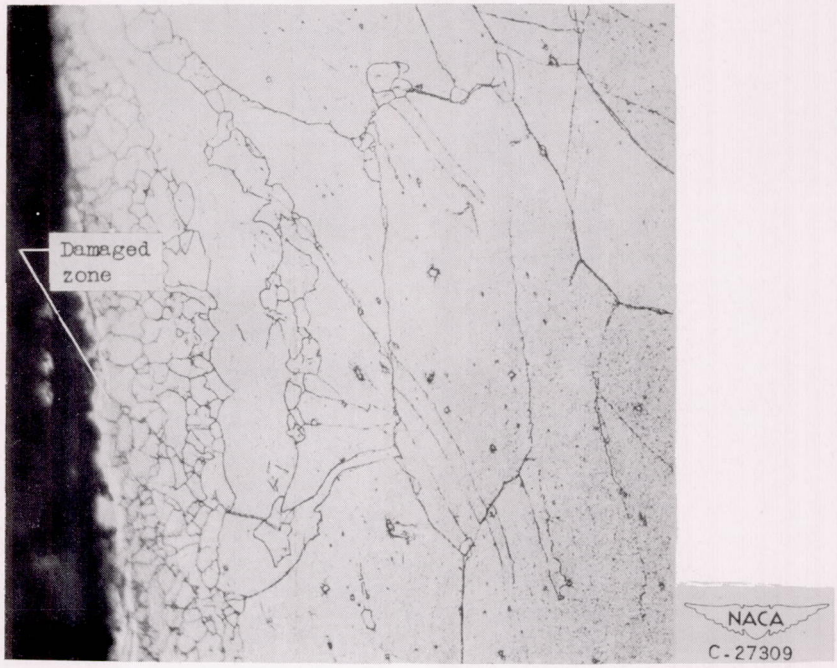


Figure 17. - Recrystallization as result of overheating at zone of damage in Inconel X blades. Electrolytically etched in 10-percent chromic acid; X250.

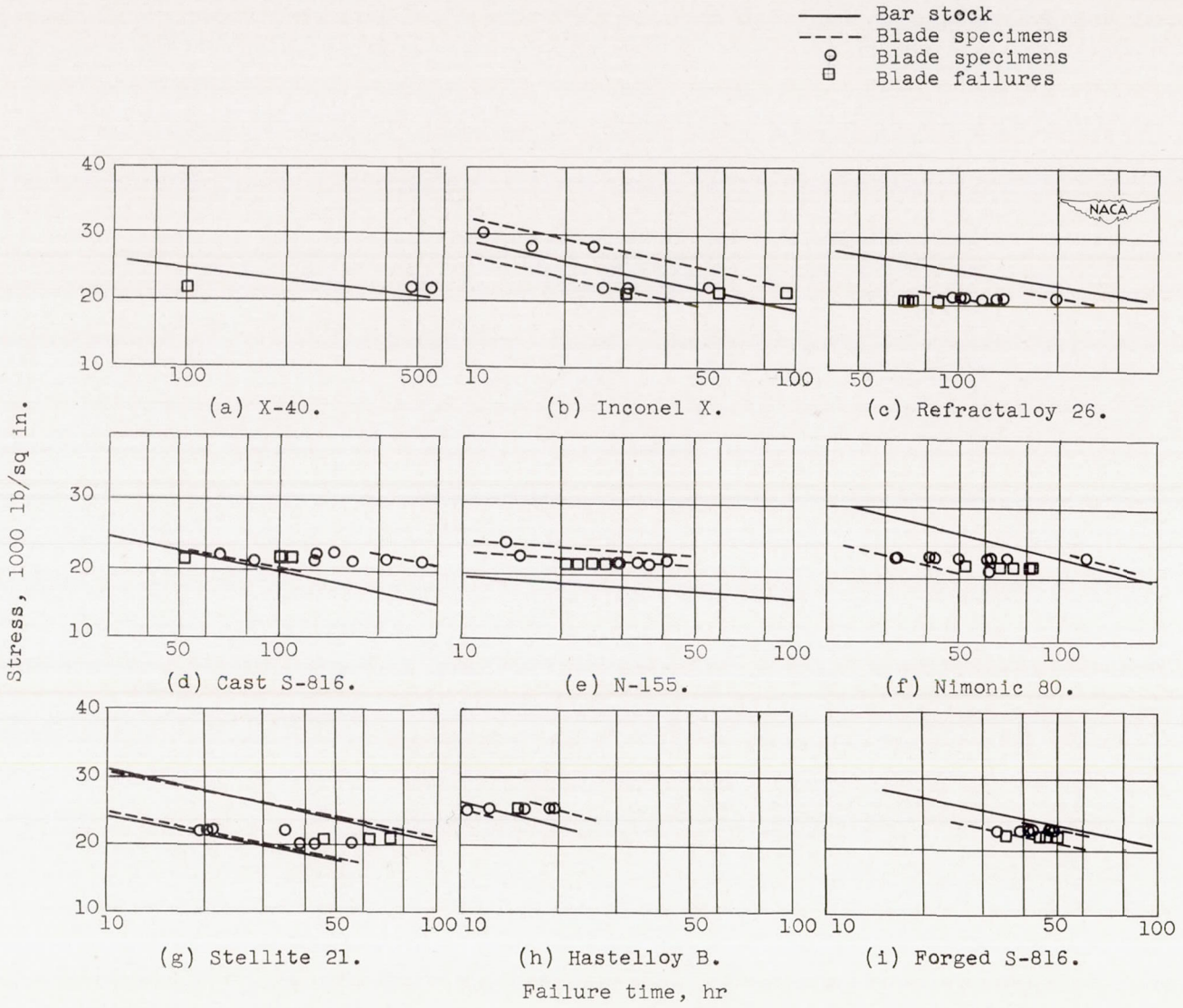
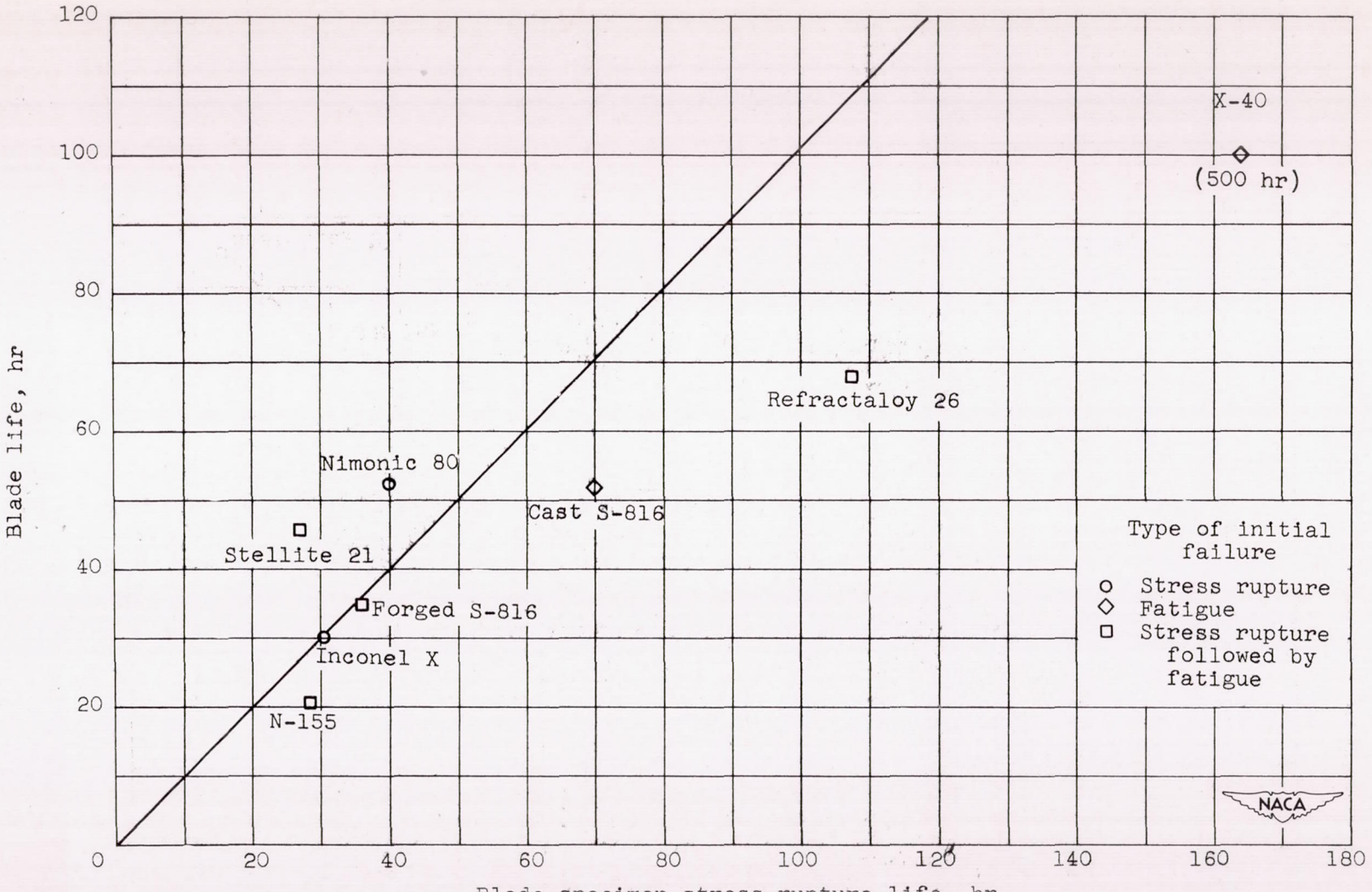
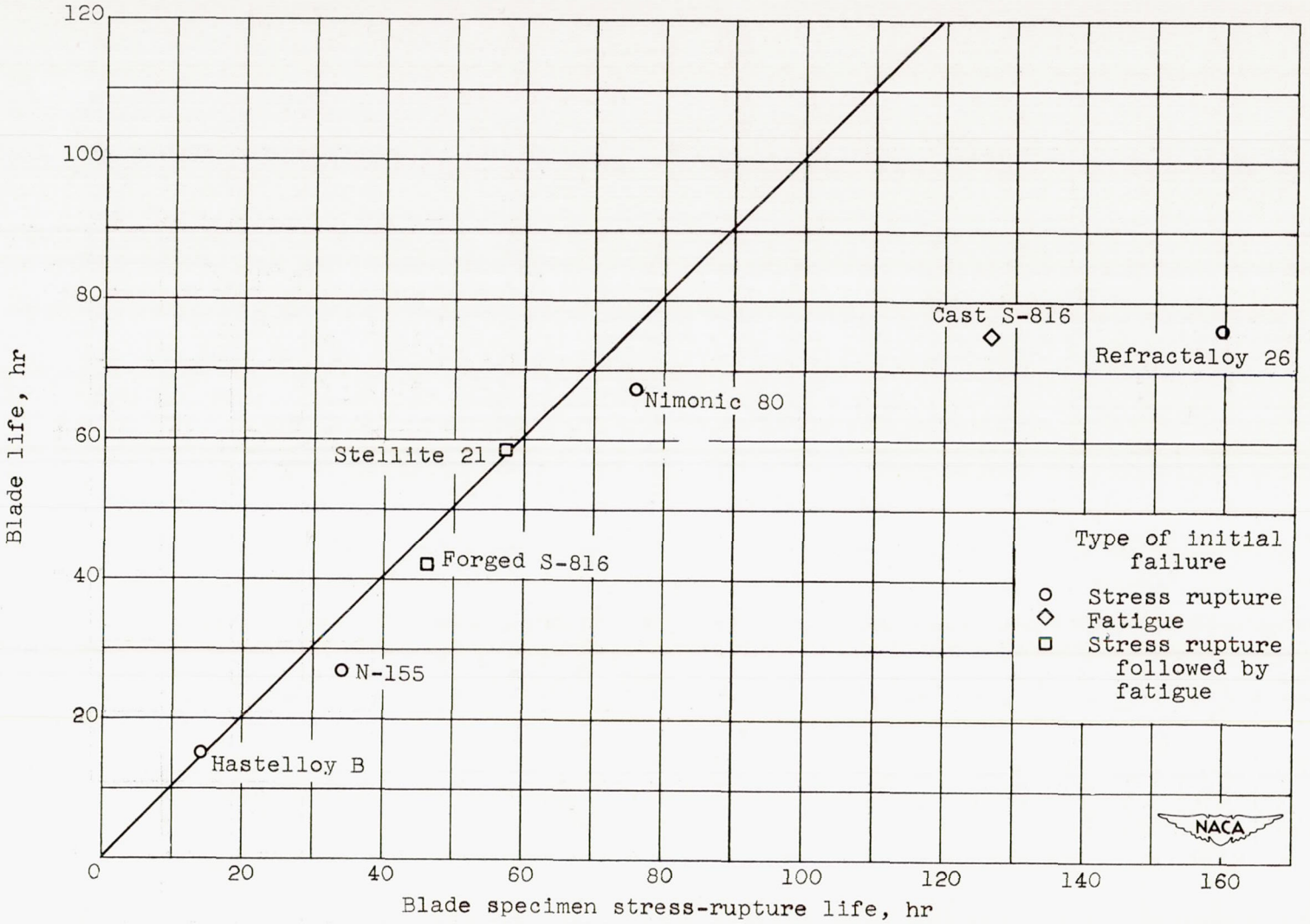


Figure 18. - Comparison of results of stress-rupture and engine investigation.



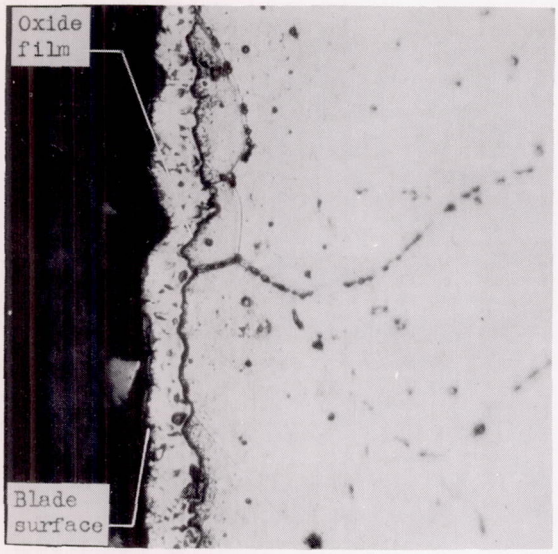
(a) Based on minimum life.

Figure 19. - Relation of blade life to stress-rupture life.

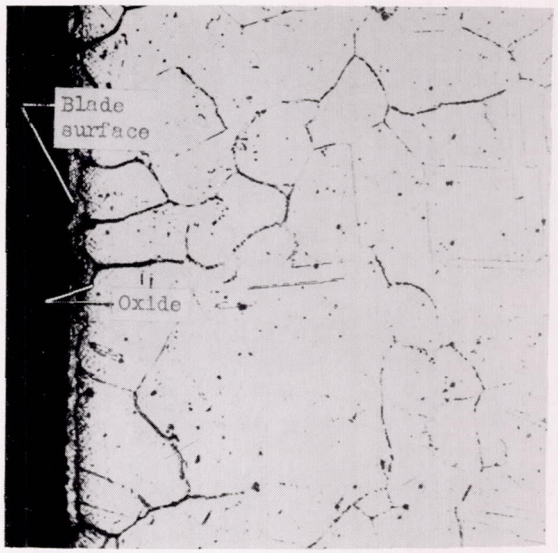


(b) Based on average data taken at midpoint of failure band.

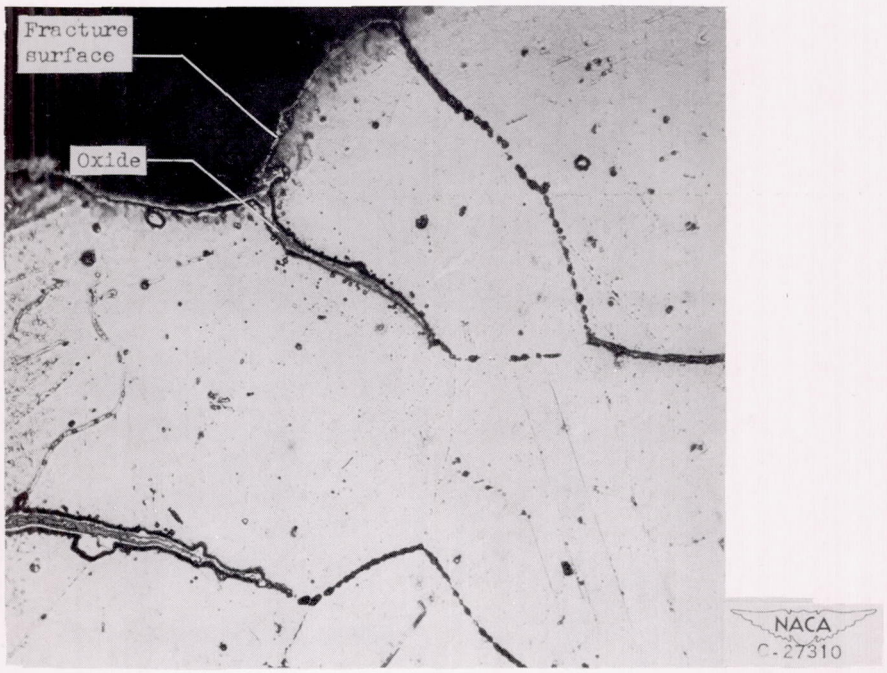
Figure 19. - Concluded. Relation of blade life to stress-rupture life.



(a) Oxide film on blade surface; X250.



(b) Intergranular penetration of oxide on blade surface; X100.



(c) Oxide in grain boundaries and along fracture surface; X250.

Figure 20. - Oxide penetration of Refractaloy 26 during engine operation. Electrolytically etched in 10-percent chromic acid.